GRAPHICAL ABSTRACT

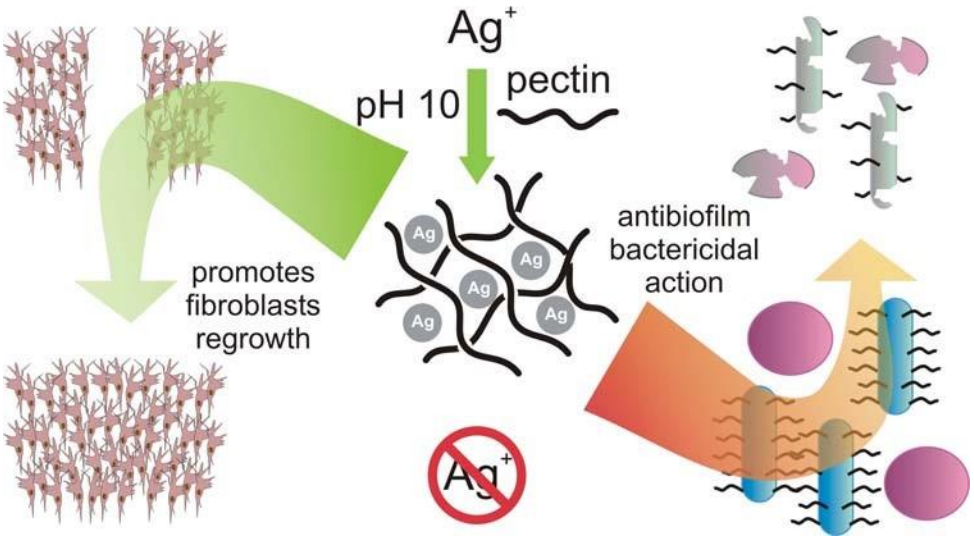

Silver nanoparticles synthesized and coated with pectin: an ideal compromise for anti-bacterial and anti-biofilm action combined with wound-healing properties

P. Pallavicini,[a]* C. R. Arciola,[b,c] F. Bertoglio,[d] S. Curtosi,[a] G. Dacarro,[a] A. D'Agostino,[a] F. Ferrari,[e] D. Merli,[a] C. Milanese,[a] S. Rossi,[e]* A. Taglietti,[a] M. Tenci,[e] and L. Visai[d,f]*

a) Department of Chemistry, Centre for Health Technologies (CHT), University of Pavia, Pavia, Italy; b) Research Unit on Implant Infections, Rizzoli Orthopaedic Institute, Bologna, Italy; c) DIMES, University of Bologna, Bologna, Italy; d) Molecular Medicine Department, Centre for Health Technologies (CHT), UdR INSTM, University of Pavia, Pavia, Italy; e) Department of Pharmaceutical Sciences, Centre for Health Technologies (CHT), University of Pavia, Pavia, Italy; f) Department of Occupational Medicine, Toxicology and Environmental Risks, S. Maugeri Foundation, IRCCS, Pavia, Italy.

Corresponding author: Piersandro Pallavicini, Department of Chemistry anc CHT, University of Pavia, viale Taramelli, 12 – 27100 Pavia, Italy; +39 0382 987336; piersandro.pallavicini@unipv.it

ABSTRACT

The synthesis of Ag nanoparticles from Ag^+ has been investigated, with pectin acting both as reductant and coating. ~100 % Ag^+ to Ag(0) one-pot conversion was obtained, yielding p-AgNP, i.e. an aqueous solution of pectin-coated spherical Ag nanoparticles (d = 8.0±2.6 nm), with a <1 ppm concentration of free Ag^+ cation. Despite the low free Ag^+ concentration and low Ag^+ release with time, the nature of the coating allows p-AgNP to exert excellent antibacterial and antibiofilm actions, comparable to those of ionic silver, tested on *E. coli* (Gram-) and *S. epidermidi*s (Gram+) both on planctonic cells and on pre- and post-biofilm formation conditions. Moreover, p-AgNP were tested on fibroblasts: not only p-AgNP were found to be cytocompatible but also revealed capable of promoting fibroblasts proliferation and to be effective for wound healing on model cultures. The antibacterial activity and the wound healing ability of silver nanoparticles are two apparently irreconcilable properties, as the former usually requires a high sustained Ag^+ release while the latter requires low Ag^+ concentration. p-AgNP represents an excellent compromise between opposite requirements, candidating as an efficient medication for repairing wounds and/or to treat vulnerable surgical site tissues, including the pre-treatment of implants as an effective prophylaxis in implant surgery

KEYWORDS: Silver nanoparticles; Anti-infective biomaterials; Biofilm; Wound healing; Silver Cation

1.INTRODUCTION

The synthesis of silver nanoparticles (AgNP) is an easy process thanks to the noble metal nature of this element. A plethora of reductants is able to transform Ag^+ in Ag(0), typically from $AgNO_3$. Borohydride, hydrazine, ethylene glycol are widely employed examples.[1] Anions (e.g. citrate), small neutral molecules (e.g. amines) or polymeric species[1,2] (e.g. polyols) may instead stabilize AgNP by adhering to their crystal faces, thus forming a coating layer that prevents aggregation by electrostatic

or steric repulsion. If AgNP are to be used for biomedical purposes, one must avoid any possibile toxicity brought by the oxidation product of the reductant, by the reductant excess and by the coating agent. In this perspective, several green syntheses of AgNP have been recently published. These are based on natural, biocompatible products[3-6] such as plant extracts, that contain mixtures of molecular species capable of reducing Ag^+, like alkaloids, proteins, polysaccharides, enzymes, alcohols, aminoacids, quinones. Due to their rich composition, plant extracts may also contain molecular species acting as coating agents, so that stable AgNP colloidal solutions are obtained in one step. However, the complexity of such extracts may lead to shape mixtures and to a large size-distribution of the obtained nanoparticles in addition to poor reproducibility, as the latter depends heavily on the origin, preparation and pre-treatment of the plant extract. This collides with the prerequisite of definite shape and narrow dimensional distribution of nanoparticles intended for pharmaceutical and medical use. We have been developing antibacterial and antibiofilm biocompatible AgNP since almost ten years e.g. by coating AgNP with cysteine and glutathione after BH_4^- reduction of aqueous $AgNO_3$. In that case excess borohydride and borates were removed by pH-controlled precipitation of the coated AgNP.[7] We have also obtained antibacterial monolayers of uncoated AgNP by their adhesion on bulk glass surfaces bearing monolayers of trialkoxysilanes terminated with -SH or $-NH_2$ groups, followed by repeated washing.[8] We are now seeking a simpler one-step synthesis, capable to yield stable AgNP in a liquid biocompatible medium that allows direct application to sensitive surfaces such as prostheses, internalized medical devices, skin burns and wounds. The latter case is particularly interesting, as beside protecting wounds from infections, AgNP were recently demonstrated to be also capable of promoting wound healing when topically delivered,[9-11] with enhanced epidermal re-epithelialization.[12] On the other hand, as fibroblasts proliferation is a requisite in wound healing processes, unreacted Ag^+ from the reduction process or Ag^+ released from the obtained AgNP must be kept at very low concentrations, as this cation is cytotoxic for eukaryotic cells.[13] To give a quantitative threshold, fibroblasts viability was recently reported to be reduced to 35 % in 10 ppm Ag^+.[14] Summarizing, an ideal AgNP colloidal solution for biomedical use should be prepared with a narrow dimensional distribution from a biocompatible reductant, that is also capable to coat and protect AgNP from aggregation, in a process where the starting Ag^+ is fully converted into Ag(0) and Ag^+ is released from AgNP only in small quantities (eg < 10 ppm), at least in 1-24 hours range. The latter is a reasonable timescale both for topical applications on wounds and for the protection against biofilm formation on implanted devices.[15] It has to be stressed that nanomechanical antibacterial action can also be obtained if a direct contact of AgNP with bacterial membranes is allowed.[7,16] This

requires a coating that weakly interact with the AgNP and such property should be ideally implemented in the chosen reductant/coater.

Most of these features can be found in pectin. Pectin is a natural polysaccharide from fruit extracts, consisting mainly of chains of D-galacturonic acid units joined by glyosidic linkages (see Figure 1),[17] although a more detailed description should include minor amounts of covalently attached rhamnose and branches of L-arabinose, D-galactose, Dxylose, and L-rhamnose.[18] The D-galacturonic acid units are naturally esterified with methyl groups, usually to a small extent (< 10%). The remaining carboxylic acidic functions have a collective pKa in the 3.5-4.1 range.[19,20] The alcoholic functions of the galacturonic units are efficient Ag^+ reductants, as it has been shown in the synthesis of AgNP.[21,22] We reasoned that by choosing a proper pectin/Ag^+ ratio full $Ag^+ \rightarrow Ag(0)$ could be obtained, at the same time mantaining an excess of –COOH groups. In such case, stabilization of the formed AgNP is expected from such groups, that are in their carboxylate form over pH 5.[23-26] Moroever, also the unreacted –OH functions can contribute to AgNP surface stabilization, as found e.g. in the case of PVA and other polyols.[1,2] A visualization of the planned working scheme is sketched in Figure 1. Finally, if using an excess of pectin, unreacted CH-OH groups would mantain a reductive environment, that is expected to minimize AgNP oxidation and Ag^+ release.

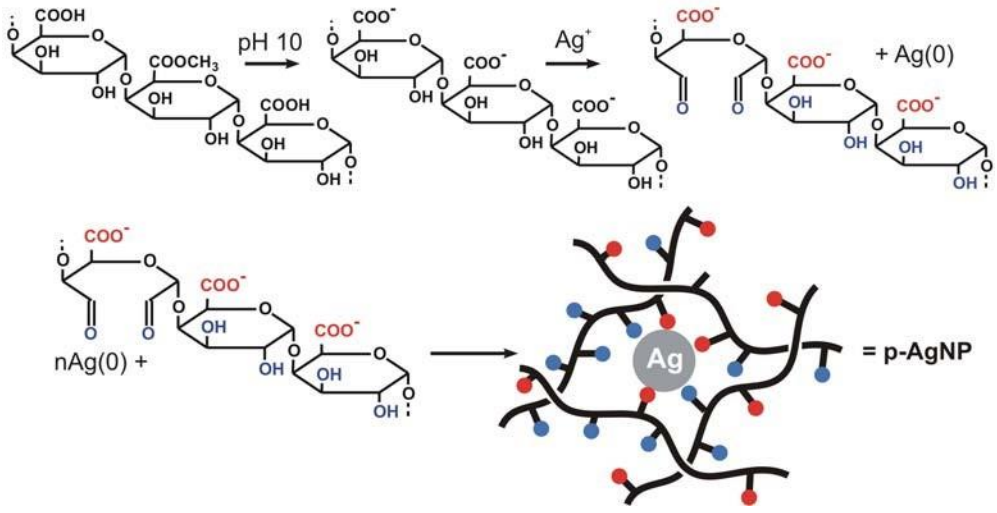

Figure 1 Working and reaction scheme for pectin/Ag^+ reaction at basic pH. The blue circles in the lower sketch represent alcoholic and aldehyde functions, red circles represent carboxylates

On this basis, in this study we have used commercial pectin from citrus peel, with low ester content (methoxy groups ≥ 6-7 %, galacturonic acid ≥ 74%) and determined the optimal pH, T and concentration conditions to obtain a highly reproducible full conversion of $AgNO_3$ into a pectin-stabilized colloidal solution of spherical AgNP (named p-AgNP), with a narrow dimensional distribution and residual Ag^+ < 1ppm. The stability of p-AgNP and their Ag^+ release with time were

also investigated using absorption spectroscopy, dialysis and quantitative Ag analysis by ICP-OES (inductive coupled plasma optical emission spectroscopy), finding that the released Ag^+ after 24 h is well below the 10 ppm threshold. On the other hand, p-AgNP demonstrated good antibacterial properties: the MIC (minimum inhibitory concentration) of p-AgNP for *Escherichia coli* PHL628 (*E. coli* PHL628, Gram -) and *Staphylococcus epidermidis* RP62A (*S. epidermidis* RP62A, Gram +) was determined and compared with that of Ag^+ (from $AgNO_3$). Since the two bacterial strains are biofilm producers, their viability in biofilm was tested, both with the bacteria plated in the presence of p-AgNPs in the medium (pre-biofilm formation) and with the biofilm produced in the absence of p-AgNPs, which were added in a second step (post-biofilm formation), with excellent results. Finally, we also verified the expected biocompatibility of p-AgNP towards fibroblasts, finding their additional capability to improve human fibroblast proliferation.

2. MATERIALS AND METHODS

2.1 Materials for p-AgNP synthesis

Pectin from citrus peel, silver nitrate, sodium chloride, hydrochloric acid (37%), sodium citrate, sodium bromide, sulphuric acid (96%), sodium hydroxide, ethanol (95%) were all purchased from Sigma-Aldrich and used without further purification. Water was bidistilled from deionized water prior to use.

2.2 Syntheses

The glassware used in all the syntheses was pre-treated by filling it with *aqua regia* and then washing it three times with bidistilled water in an ultrasound bath for 5 minutes.

AgNP from pectin solution (p-AgNP). Pectin from citrus peel was dissolved in 50 mL bidistilled water to form 0.5%, 1% and 2% (w/w) solutions. Complete dissolution was obtained by magnetic stirring at 60 °C for 20 minutes. The solution was then cooled at room temperature and the calculated volume of an $AgNO_3$ 0.1 M aqueous solution was added to obtain final Ag^+ concentration = 0.001M or 0.01 M. Then, standard 0.5 M NaOH solution was immediately added to obtain 0.025 M OH^- (measured pH = 10.5-11.0). Such a mixture was kept under vigorous magnetic stirring for 12 hours either at 60 °C and for 24 h at RT (20 °C). After 10-15 min a yellow brown color started to appear, that increased in intensity with time. After this, yellow-brown colloidal solutions of AgNP (p-AgNP) were obtained, that were kept in a stoppered flask at RT and used with no further treatment.

Dry p-AgNP. 9.0 mL of 95% ethanol were added to 1.0 mL of p-AgNP solution observing a quick turbidity formation. The mixture was then ultracentrifuged at 13000 rpm (15870 g) for 60 minutes, obtaining a brown dense suspension at the bottom of the test-tube (1.5 ml volume) and a colorless

supernatant. The latter was removed and the remaining suspension transferred in an Eppendorf vial (2.5 mL) and further ultracentrifuged at 13000 rpm (17760 g) for 20 + 20 minutes. After each time slot the supernatant was removed, ending with a wet brown precipitate of < 0.2 mL, that was dried first in a N_2 flux for 1h, then overnight in a vacuum desiccator.

2.3 Chemical and physical-chemical methods.

Determination of Ag^+ content in the p-AgNP solutions. The Ag^+ content in the p-AgNP colloidal solutions was determined by potentiometric titration, using the standard addition method.[27] A combined silver electrode consisting of a silver bar (diameter 8 mm) and a Mercury/Mercurous Sulfate (Hg/Hg_2SO_4, saturated K_2SO_4) reference electrode were used (Radiometer Analytical, code MC6091Ag-9). Measures were performed with a Haita model 903 potentiometer, with a precision of ± 0.1 mV. Prior of the analysis, KNO_3 was added to the samples as a supporting electrolyte, so that the final solution was 0.1 M with respect to this salt. A calibration line was built by adding known amounts of silver nitrate (from 0.1 up to 200 mg/L) to 0,5%, 1% or 2% w/w pectin solution in 0.1M KNO_3, and plotting log [Ag^+] vs E (mV). A straight line with a Nernstian slope (ca 60 mV for ten-fold change in concentration) was always obtained (SI5). The entire operation was carried out at 20°C in less than 20 min and in the absence of added base, to avoid reduction of silver by pectin.

Other methods. Ag^+ release studies, Differential scanning calorimetry (DSC) and thermogravimetric analysis (TGA), X-ray diffraction, TEM imaging, Dynamic Light Scattering (DLS) and Z-potential were carried out according to standard procedures, that are described in detail in the Supporting Material (SI-Details on experimental methods)

2.4 Antibacterial and antibiofilm studies

Bacterial strains and culture condition. The microorganisms used in this study, *Escherichia coli* PHL628 and *Staphylococcus epidermidis* RP62A, are biofilm-producing strains. *E. coli* PHL628 was provided by Dr Roberta Migliavacca (University of Pavia, Italy) whereas S. *epidermidis* RP62A was a kind gift from Prof Timothy J. Foster (Department of Microbiology, Dublin University, Ireland). A starter culture of *E. coli* PHL628 or *S. epidermidis* RP62A was grown overnight, respectively in Luria Bertani Broth (LB) and in tryptic soy broth (TSB) (Difco Laboratories Inc., Detroit, MI, USA), under aerobic conditions at 37 °C using a shaker incubator (Certomat® BS-T, B.Braun Biotech International, Melsungen, Ger) at 200 rpm.

Evaluation of antimicrobial activity of p-AgNPs and $AgNO_3$. Prior to any use, p-AgNPs were sterilized at 60°C for three hours and filtered through 0.45µm filter membrane to eliminate possible precipitated pectin. Instead, $AgNO_3$ was filter-sterilized (0.22 µm).

Planktonic bacterial culture conditions - To determine the Minimum Inhibitory

Concentration (MIC) of the generated p-AgNPs suspensions and $AgNO_3$ in planktonic conditions, overnight starter cultures were diluted in appropriate fresh medium to 1 x 10^4 bacteria/ml by comparing the OD_{600} of the overnight culture with a standard curve correlating OD_{600} to bacteria number. Geometric dilution of p-AgNPs suspensions or $AgNO_3$ were performed starting from the initial concentration of 1 mM for successive ten 1:10 dilution in 100 µl. Then, 100 µl of the diluted bacterial suspension was added to the microtiter plate and incubated for the indicated times at 37°C in static conditions. Bacteria viability was estimated through the quantitative 3-[4,5-dimethylthiazol-2-yl]2,5diphenyltetrazoliumbromide (MTT) (Sigma Aldrich, St.Louis, MO, USA) test.[20][28] This colorimetric assay measures dehydrogenase activity as an indicator of the bacterial metabolic state. Briefly, 5 mg/mL of MTT solution, dissolved in PBS (0.134 M NaCl, 20mM Na_2HPO_4, 20 mM NaH_2PO_4), was used as stock solution and the working concentration was 0.5mg/mL. The test was performed at 37°C for 3 hours. Upon presence of viable bacteria, reduction of the MTT salt results in purple insoluble formazan granules that are dissolved in acidified 2-propanol (0,04 N HCl). The result was recorded through an iMark® Microplate Absorbance Reader (Bio-Rad, Hercules, CA, USA) at 562 nm with the reference wavelength set at 655nm. Cell survival was expressed as percentage of the number of bacteria treated with p-AgNPs or $AgNO_3$ to the number of bacteria grown in absence of any treatment.

Bacterial biofilm culture conditions - Bacterial viability in biofilm-forming conditions was evaluated as follows: the overnight starter culture was diluted in 0.25% glucose-containing medium to induce biofilm formation. *E. coli* PHL628 was diluted at a final ratio of 1: 100 and *S. epidermidis* RP62A at 1:200. Pre-biofilm conditions: geometric dilutions of pAgNPs suspensions or $AgNO_3$ in glucose-enriched medium were incubated with 100 µL of bacterial suspension for 24 hours as previously described. Post-biofilm conditions: biofilm was allowed to form for 24 hours at 37°C. The supernatant, containing planktonic bacteria, was carefully removed and p-AgNPs suspensions or $AgNO_3$ already diluted in the appropriate medium were added to the formed biofilm and incubated for further 24 hours. In both culture conditions, at the end of the incubation period, biofilm was vigorously suspended by pipetting and scratching. The viability was assessed through MTT assay as previously described. Experiments were performed in triplicate.

Confocal Laser Scanning Microscopy (CLSM) studies. Methods for CLSM are described in detail in the Supporting Material (SI – Details on experimental methods) **2.5 In vitro cytotoxicity and cell proliferation studies In vitro cytotoxicity and cell proliferation studies**

Materials. Dimethyl sulfoxide, Dulbecco's Phosphate Buffer Solution, MTT (3-(4,5dimethylthiazol-2-yl)-2,5-diphenyltetrazolium bromide), Antibiotic Antimycotic Solution (100×; stabilized with 10,000 units penicillin, 10 mg streptomycin and 25 µg amphotericin B per mL), trypan blue solution,

trypsin–EDTA solution, Hank's balance salt solution (HBSS), all purchased from Sigma-Aldrich, were used. Dulbecco's Modified Eagles Medium (DMEM) was purchased from Lonza BioWhittaker (Walkersville, USA), and inactivated foetal calf bovine serum from Euroclone (Milano, Italy).

NHDF fibroblast cell culture. Cell culture methods for NHDF fibroblasts are described in the SUPPORTING MATERIAL (SI – Details on experimental methods)

Assessment of fibroblast viability in presence of p-AgNPs suspension. The effects of p-AgNP on the viability of human fibroblasts were investigated. Cells were seeded on 96-well plates (3.5 10^4 cells in 200 μl of complete medium/well) and left in incubator for 24 h in order to reach confluence. PEC aqueous solution (1% w/w) and p-AgNP suspension were diluted (1:10, 1:20 1:40 v/v) in medium without fetal bovine serum (M (w/s)) and 200 μl of each sample was put in contact for 24 h with cells. Complete medium (CM) and medium without fetal bovine serum (M (w/s)) were used as references. After incubation, samples were removed from the plate well and 50 μl of MTT (3-(4,5-dimethylthiazol-2-yl)-2,5diphenyltetrazolium bromide) 7.5 μM in 100 μl of HBSS (pH 7.4) was added to each well and incubated for 3 h. Finally, 100 μl of a solubilization solution (dimethyl sulfoxide) was added to each well, and mixed with the cells to allow the complete dissolution of formazan crystals, obtained from the reduction of the dye MTT into cells by dehydrogenase enzyme. The solution absorbance was determined at a wavelength of 570 nm, with a 690 nm reference wavelength, by means of an IMark® Microplate reader (Bio-Rad Laboratories Srl, Segrate, Milan, Italy) after 60 s shaking. Results are expressed as % viability, normalizing absorbance measured after contact with samples with that measured after contact with M (w/s). Eight replicates were performed for each sample.

Assessment of cell proliferation properties of p-AgNPs suspension. The capability of p-AgNP to improve NHDF fibroblasts growth was also evaluated. Cells were seeded on 96well plates (2×10^4 cells in 50 μl of M w/s / well) and immediately put in contact with pAgNP suspension (200 μl) for 24 h. The sample was diluted 1:10, 1:20 and 1:40 v/v in M (w/s). M (w/s) was used as reference. At the end a MTT test was performed (as described in the previously paragraph).

Wound healing test. The in vitro wound-healing test is based on the employment of a Petri μ-dish (35 mm, Ibidi, Giardini, Milan, Italy) in which an insert is enclosed. The insert is constituted of two chambers with a growth area of 0.22 cm^2 divided by a septum, mimicking the lesion area, with a width of 500 μm ± 50 μm. Fibroblasts were seeded in each chamber at 10^5cells/cm^2 and growth at confluence in standard conditions as above mentioned. After 24 h, cells reached confluence and the insert was removed, displaying two areas of cell substrate divided by the prefixed gap. Cell substrates were put in contact with 400 ml of pAgNP diluted 1: 20 v/v with M(w/s). Wound healing test was also performed on M (w/s) and CM, used as references. At prefixed times (24, 48 and 72h)

microphotographs were taken to evaluate the invasion and cell growth in the gap. At each time the maximum value of gap width was measured. Three replicates were performed for each sample.

Statistical analysis. Whenever possible, experimental values of the various type of measures were subjected to statistical analysis, carried out by means of the statistical package Statgraphics 5.0 (Statistical Graphics Corporation, Rockville, MD, USA). In particular, Anova one way- Multiple Range Test was used.

3. RESULTS AND DISCUSSION

3.1 Synthesis of p-AgNP.

The synthesis of colloidal solutions of AgNP stabilized by pectin (p-AgNP) was carried out using 0.5, 1.0 and 2.0 % w/w pectin solutions in bidistilled water. $AgNO_3$ was added from a concentrated aqueous solution to obtain final Ag^+ concentrations of 0.001M or 0.01 M. Reaction did not start until base was added to a concentration of NaOH of 0.025 M. The measured pH was 10.5-11.0, depending on pectin concentration. Temperature was kept at 20 °C or 60 °C, with vigorous stirring on a magnetic stirrer. Ag reduction to p-AgNP started within 5 minutes after base addition and it was visually perceivable by the appearance of a yellow color, turning soon into the characteristic deep yellow-brown of AgNP. The reaction was quantitatively followed by measuring the absorption spectra of the reaction mixture, in which the typical localized surface plasmon resonance (LSPR) of AgNP was observed. In the case of 0.001 M Ag^+ the LSPR band maximum was at 409-416 nm under all conditions (see Table 1). The intensity of the LSPR absorption band increased during the first reaction hours, reaching a limiting value within 24 h at 20 °C and within 6 hours at 60 °C. Figure 2 reports the series of absorption spectra recorded in the case of 0.001 M Ag^+ at 20 °C and 60 °C in 0.1 % pectin. Representative absorption spectra at 24h and 5-14 days (as a stability control) are reported in the Supporting Material (SI1) for preparations with 0.001 M Ag^+ with all the used pectin concentrations, both at 20 °C and 60 °C. Nanoparticles dimensional analysis was carried out on all preparations using transmission electron miscroscopy (TEM, see Figure 2E and SI2). With 0.001 M Ag^+ spherical NP were observed with a ~ 8 nm average diameter, see Table 1. A narrow dimensional distribution was found (standard deviations are 2-3 nm) as confirmed also by the sharp shape of the LSPR bands, see Figure 2A, C and SI1. Also band widths at half height were small, i.e. in the 61-69 nm range (Table 1), and no shoulders were observed at $\lambda > 450$ nm, neither at 24h nor after several days after preparation (SI1), evidencing that no aggregation or unsymmetrical NP growth took place.

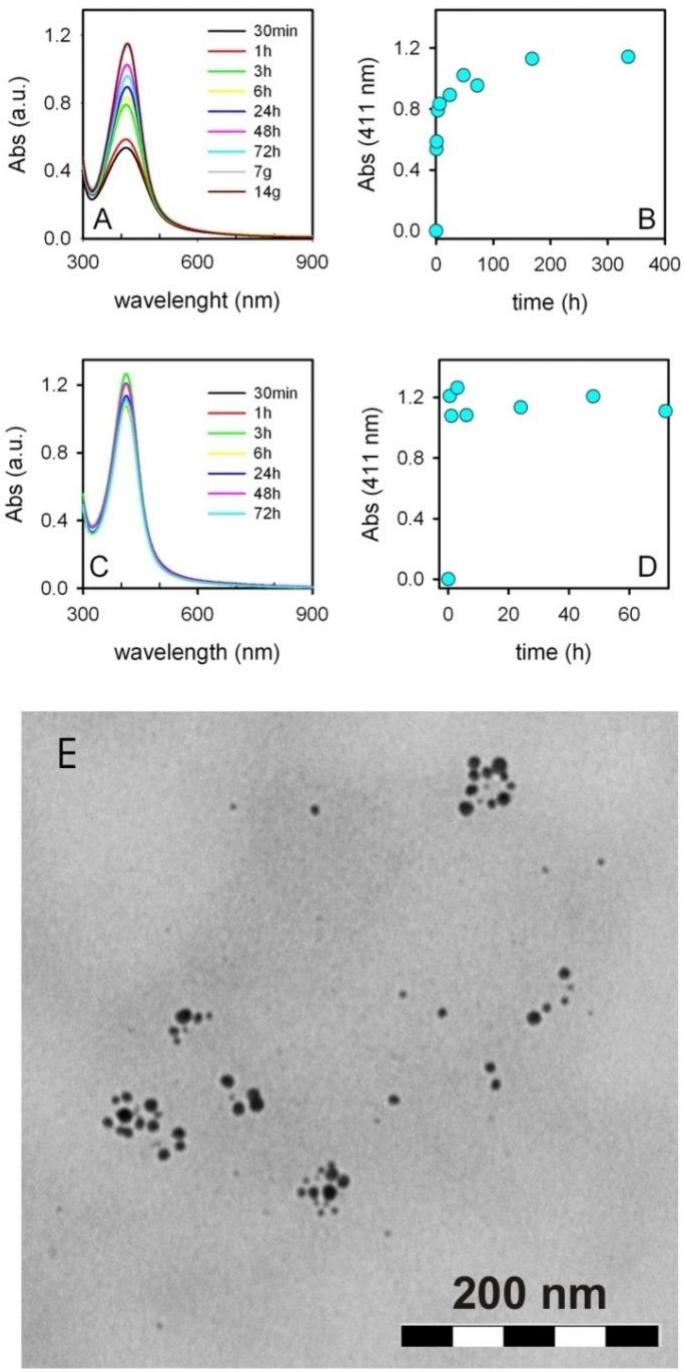

Figure 2. **A** and **C**: series of absorption spectra in a solution of 1% pectin/Ag^+ at basic pH, at 20 °C (panel A) and at 60 °C (panel C); the time at which spectra were taken can be read by the color in the inset list. **B** and **D**: absorbance at the LSPR maximum (411 nm) vs time, obtained from the spectra of panel A and C, respectively. **E**: TEM image obtained from a preparation with 1% pectin/Ag^+, 60 °C

Formation of AgNP was efficient also at higher Ag^+ concentration, namely 0.01 M Ag^+, with slightly higher maximum absorption wavelength (415-420 nm) observed with preparations carried out with 0.5-2% pectin at 20 and 60 °C. However, in this case spectral (SI3) and dimensional (SI4) TEM characterization revealed a slower transformation of Ag^+ into AgNP and a larger dimensional distribution, including the presence of large aggregates and non-spherical objects. As an example

Figure ESI3A and ESI3B show that with 0.5% pectin and 20 °C the p-AgNP formation is not complete even after 14 days, with a band width at half height at such time of 96 nm. These results discouraged us from further use of such silver-rich preparations. On the other hand, all the preparations with 0.001M Ag^+ seemed feasible for use in biomedical treatments, due to their reproducibility, narrow dimensional distribution and fast preparation time.

% pectin	AgNP diameter (nm)[a]		LSPR band, λ_{maxb}(nm)	
	20 °C	60 °C	20°C	60 °C
0.5	8.3 (3.0)	8.0 (3.6)	411(68)	409(63)
1.0	8.8 (3.5)	8.0 (2.6)	412(69)	412(63)
2.0	8.4 (3.4)	8.0 (3.6)	411(63)	416(61)

Table 1. Dimensional and optical data for p-AgNP prepared with 0.001M $AgNO_3$. [a]standard deviation in parenthesis; [b]width at half height (nm) in parenthesis

We decided to use the preparation with 1.0 % pectin and 60 °C as our synthesis of choice, due to short completion time and best stability after preparation. As it is shown in Figure SI1D, the absorption spectra carried out at 1d and 14d are perfectly superimposable, while preparations with 0.001 M and 0.5 or 2.0% pectin showed slight increases of the band width at half height after 14d. Finally, the chosen synthetic conditions also assure high reproducibility, as it can be seen from the superimposition of absorption spectra from different preparations (Figure SI1G). The starting base concentration of 0.025 M NaOH was also used as a standard, as less basic conditions led to slower reaction or uncomplete $Ag^+ \rightarrow$ Ag(0) conversion. The final pH after reaction completion was in all preparations in the 8.4-8.8 range. We also controlled the p-AgNP stability under three conditions on the 0.1% pectin 60 °C product: i) NaCl added as a solid at a 0.1 M concentration; ii) 0.1M HCl added until pH 5.0 was reached; iii) a 1:1 v/v mixture with PBS (phosphate saline buffer, pH 7.4). In all cases no precipitation or turbidity was observed, with the shape of the LSPR band remaining unchanged under absorption spectra examination after 8 h. Finally, we examined the conversion yield of Ag^+ to Ag(0) in the preparations with 0.001 M Ag^+, 0.5-2.0% pectin and T = 20 °C and 60 °C. Attempts to separate p-AgNP from the solvent by ultracentrifugation were unsuccessful (13000 rpm), and this prevented the use of the simpler technique, i.e. analysing free Ag^+ in the supernatant. We used instead an electrochemical method elaborated on purpose, see full details in the Experimental.

Briefly, potentiometric measurements of free Ag^+ were carried out with the standard additions technique. A calibration curve was calculated using the same pectin concentrations as in the syntheses and adding measured Ag^+ quantities. In the case of the calibration curve, measurements were carried in few minutes (< 5) after additions and with no added base, to rule out any p-AgNP formation (no yellow color was noticed under these conditions). When examining the free Ag^+ found in p-AgNP preparation after 12 h reaction time, a concentration ≤ 1 ppm was found in all cases, corresponding to ≤ 1% of the overall starting Ag^+, i.e. a complete conversion (> 99%) was obtained for 0.001M Ag^+ in 0.5-2.0% pectin. In particular, in the preparation with 0.001 M Ag^+ and 1.0% pectin at 60 °C, 0.79 ppm (7.38×10^{-6} mol/L) of free Ag^+ were found, corresponding to the 0.74% of the total Ag. Additional material on potentiometric analysis and a Table with full data are in SI5. Such data strongly support the possibility of using p-AgNP in regenerative processes such as wound healing, as the concentration of free Ag^+ is well below the values leading to cytotoxic effects on fibroblasts.[14]

3.2 Reaction mechanism and product characterization.

The qualitative reaction mechanism of the synthesis was investigated by FT-IR spectroscopy. The spectrum of commercial pectin powder (Figure 3A, black) shows a carbonyl absorption band at ~ 1735 cm^{-1} that is due both to the carboxylic acid and to the ester groups of pectin. A less intense band at 1608 cm^{-1} can be attributed to the presence of some deprotonated carboxylic acid groups. Finally, a large absorption at > 3000 cm^{-1} is due to adsorbed water and to –OH stretching. Pure pectin (1% w/w) was treated with base (NaOH 0.025 M, pH 10.5-11.00) for 6 h at 60 °C, then isolated as described in the experimental (briefly: precipitation by 1:10 dilution in ethanol, followed by ultracentrifugation). In its FT-IR spectrum (Figure3A, red) the band at 1735 cm^{-1} has disappeared, while the band at 1608 cm^{-1} is increased. Under these conditions all the -$COOCH_3$ ester groups are hydrolyzed to –COOH, and all –COOH groups are in their carboxylate form. The FT-IR spectrum of the p-AgNP product (Figure 3B, blue), obtained with 0.001 M Ag^+, 1.0% pectin and T = 60 °C (isolated as for hydrolyzed pectin, see Experimental), is very similar to that of the pure pectin treated under the same conditions but in the absence of Ag^+. This is not surprising, as in the used synthetic conditions it may be calculated that we added 5×10^{-5} mol Ag^+, that has 2.35×10^{-3} mol of galacturonic acid available for reaction (considering, as an approximation, pectin composed only by the latter). If the secondary alcohol groups are responsible of the Ag^+ reduction, only 1/100 of the galacturonic acid units would react with Ag^+, this resulting in negligible spectral changes. To further investigate this point we run the Ag^+-pectin reaction at 60 °C also in 1:1 silver/galacturonic acid conditions, i.e. 0.5 g pectin (2.35×10^{-3} mol of galacturonic acid) in

50 mL water were reacted with 0.400 g (2.35×10^{-3} mol) $AgNO_3$, at pH 10.5.

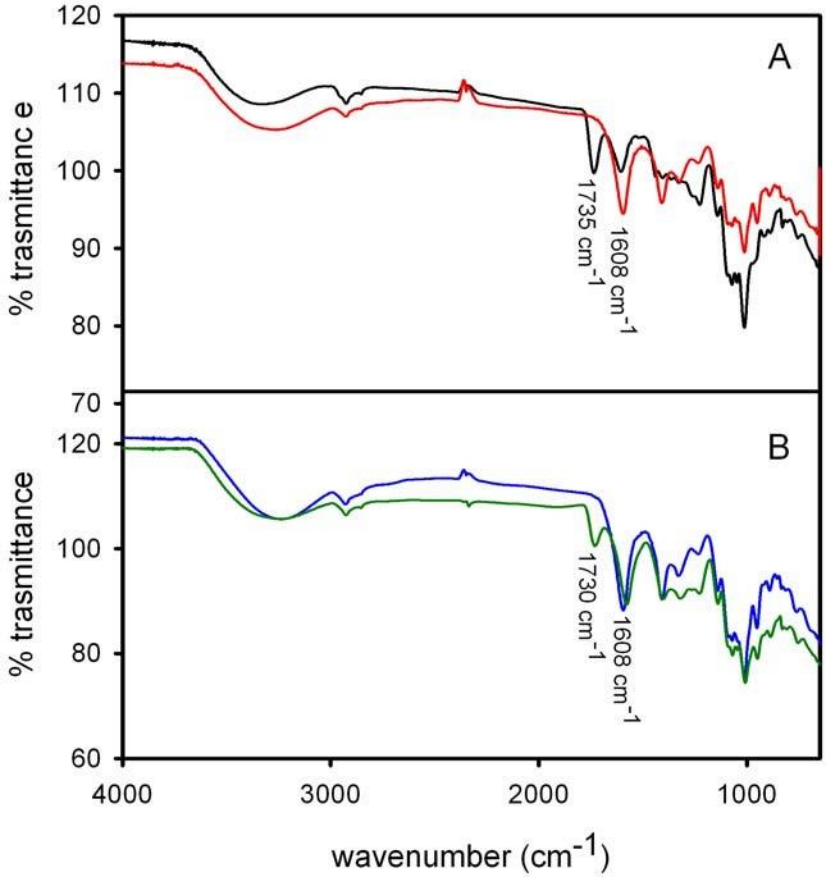

Figure 3. IR spectra. **A**: pectin as such, black; pectin after treatment at pH 12, 50 °C, red. **B**: p-AgNP product under standard synthetic conditions (Ag^+ 0.001 M, 1.0% pectin, 60°C), blue); same, but with excess Ag^+ (equimolar with galacturonic acid units), green. The wavenumber of the relevant bands are reported in the figure

Also in this case abundant formation of p-AgNP was observed, as an orange-brown slurry formed. Isolation and drying of the product with the same work up gave a powder whose FT-IR spectrum is displayed in Figure 3B, green. In this case, beside an increase of intensity of the carboxylate band and a decrease of the -OH stretching band, a band at 1730 cm^{-1} is clearly present. This may be attributed to the oxidation of the diol moiety of the galacturonic acid units to dihaldehyde, reducing Ag^+ to Ag according to the scheme described in Figure 1 and, in more detail, to Reaction (1)

$$\text{R-CH(OH)-CH(OH)-R} + 2Ag^+ \rightarrow 2\ \text{RCH=O} + 2Ag + 2H^+ \qquad (1)$$

The determination of pH before and after the synthesis completion also agrees with this reaction and with the observed hydrolysis of the ester groups. We found final pH values 8.48.8 in all preparations, starting from pH values 10.5-11.0. Attempts to prepare p-AgNP without base addition resulted in no AgNP formation.

The solid dry p-AgNP isolated from the standard preparation (1% pectin, 10^{-3}M Ag^+, 60 °C) has been examined with coupled DSC and TGA experiments (see SI6), finding 3.5% weight Ag. In the starting mixture Ag is 1.1% w/w with respect to pectin. The 3-fold increase confirms that pectin is in large excess and most of it does not interact with AgNP and is eliminated during the isolation work up. X-ray diffraction (SI7) fully confirmed the nanocrystalline nature of the p-AgNP in the pectin matrix. Debye–Scherrer analysis and Rietveld refinement found nanocrystallites dimensions of 7.5 nm, in excellent agreement with the p-AgNP dimensions determined by TEM. Dynamic Light Scattering and Z- potential measurements carried out on freshly prepared p-AgNP (0.001 M Ag^+, 1.0% pectin, 60 °C), found instead large objects with average diameters 170-180 nm and with Z potential = -50 mV. Examining the TEM images (obtained from p-AgNP solutions diluted 1:10), see Figure 2E, grouped AgNP may be distinguished, although with significant interparticle distance (in agreement with the absence of bands at $\lambda > 410$ nm), while the poorly electron dense pectin cannot be imaged with TEM. We could hypothesize that the large objects observed with the DLS technique correspond to several AgNP grouped by one or more pectin polymer chains.

3.3 Antibacterial and antibiofilm activity of p-AgNP.

The free Ag^+ concentration found after the synthesis is low (< 1 ppm), but it could be sufficient to exert an antibacterial effect. Moreover, we have already found that AgNP coated with weakly adhering molecules (such as citrate or carboxylates) exert an intrinsic mechanical antibacterial effect, due to direct contact and disruption of bacterial membranes.[7,16] Finally, amplification of the action of various antibacterial agents has been reported in the presence of pectin,[29,30] due to the delivery-promoting adhesion of the latter to bacteria membrane. On this basis, the effect of p-AgNP prepared from 1 mM Ag^+ in 1% pectin at 60 °C was tested on two different bacterial strains, *Escherichia coli* PHL628 (Gram-) and *Staphylococcus epidermidis* RP62A (Gram+). The effect was first evaluated in liquid culture conditions at various concentrations of p-AgNP. The concentration of Ag(0) in the p-AgNP solutions was assumed to be 1 mM, considering the ~100% $Ag^+ \rightarrow Ag(0)$ conversion found by potentiometric determination of free Ag^+. Successive geometric v/v dilution of p-AgNP bulk solutions with TSB allowed treatments at 500, 250, 125, 62.5, 31.25 and 15.625µM Ag concentration. The obtained MIC values are summarized in Table 2. For the complete trends of viability vs Ag concentration see SI8.

	E. coli PHL628		*S. epidermidis* RP62A	
	6h	24h	6h	24h
p-AgNP[a]	15.62 µM	31.25 µM	250 µM	500 µM

Ag^+ ($AgNO_3$)	-[b]	125 μM	-[b]	125 μM
gsh-AgNP[c]	-[b]	140 μM	-[b]	1680 μM[d]

Table 2: MIC values for p-AgNP and ionic silver in liquid culture conditions. [a]experiments were repeated two times on two different p-AgNP preparations, with identical results; [b]MIC for Ag^+ was not determined at 6h; [c]values from ref 7; [d]data obtained with *S. aureus*

MIC for p-AgNP was found to be 31.25 μM for *E. coli* PHL628 and 500 μM for *S. epidermidis* RP62A after 24 h incubation. Working on colloidal solutions of glutathionecoated AgNP (gsh-AgNP) of comparable dimensions (d = 7 nm), we previously found[7] in ISB (Iso-Sensitest Broth, Oxoid, England) at pH = 7 a MIC value of 140 μM for *E. coli* ATCC 10536 and of 1680 μM for *S. aureus* ATCC 6538, after 24 h incubation. Values are included in Table 2 for comparison. While the greater resistance of Gram+ bacteria to silver is well-known in literature[31,32] and it is confirmed in the present work, the lower MIC values found here with respect to gsh-AgNP prompted us to determine as a control the MIC of ionic silver (from $AgNO_3$ 0.001M aqueous solution) under the same experimental conditions. The MIC for Ag^+ was 125 μM for *E. coli* PHL628 and *S. epidermidis* RP62A, on colonies incubated for 24 h. Due to the used dilution method for determining MIC, it may be assumed that while 62.5 μM Ag^+ was not sufficient to fully inhibit bacteria growth for both strains, 125 μM was shown to be enough. However, the exact MIC values for both strains are comprised between 62.5 and 125 μM. These values fit well with what previously reported for *E. coli* ATCC 10536 and *S. aureus* ATCC 6538[7] as MIC values for Ag^+ (from $AgNO_3$) were 93 μM and 140 μM, respectively, after 24 h incubation time. In the present paper, the MIC at 24 h of p-AgNP for *E. coli* is noticeably lower at the same incubation time not only in comparison to the MIC of gsh-AgNP but also to the MIC of ionic Ag^+. It has to be stressed once again that negligible Ag^+ (1 ppm ≅ 9.2 μM) is present in the p-AgNP solution after synthesis, as demonstrated by potentiometric experiments. It may be argued that diluting the p-AgNP solution with TSB and allowing the contact with bacterial colonies shifts the p-AgNP system from equilibrium, inducing further Ag^+ release. To mimic such conditions, we carried out also release experiments from p-AgNP contained in a dialysis membrane immersed in an identical volume of bidistilled water (see Experimental Section and SI9 for full results): after 24 h, 1.95 Ag^+ ppm (18 μM) was found in the aqueous phase external to the membrane, corresponding to 1.9% of the silver contained in p-AgNP inside the membrane. Considering this, we can assume a role of the released Ag^+ in the antibacterial action of p-AgNP. However, it is necessary to hypothesize that on p-AgNP treatment, the hugely increased antibacterial action towards *E. coli* is connected to the AgNP

coating.[33] AgNP have no strongly stabilizing thiolate bonds on their surface like in gsh-AgNP, thus being capable to exert a direct nanomechanical disrupting action[16] on the *E. coli* membrane. At this regard, it should be mentioned that AgNP of similar dimensions (d = 7 nm) and coated with a carboxylate (deprotonated gallic acid) showed a comparable MIC of 58 μM at 12 h with *E. coli*.[34] Citrate-coated AgNP gave a lower MIC for *E. coli*, 2.3 μM, but at a much shorter incubation time, i.e. ≤ 3 h.[35] These values can be reasonably compared with the MIC measured on bacteria incubated for 6 h (Table 2), that are lower as after a shorter strains growth time less antibacterial agents are needed to inhibit the colony growth. In addition, a favourable action is plausibly played by the pectin coating: it may be suggested that the surface activity and mobility of p-AgNP and of the low-concentrated Ag^+ is amplified by the delivery-promoting action of pectin adhering to bacteria membranes.[29,30] The greater p-AgNP antibacterial efficiency over gsh-AgNP is confirmed also by the MIC comparison on *Staphylococcus* strains, although caution must be used as the two MIC values are obtained with two different staphylococcal species, namely *S. epidermidis* and *S. aureus*. However, in both cases it can be stated that the thick peptidoglycan layer of the Gram+ cell wall increases the bacteria resistance to the AgNP action, probably due to prevention of the penetration of AgNP inside the cytoplasm.

Since both *E. coli* and *S. epidermidis* strains tested for MIC determination are also biofilm producers, their viability in biofilm-forming conditions, i.e. with 0.25% Glucose (Glc) supplement in the medium, was evaluated. The investigation was performed in two setups: (i) the bacteria were plated in the presence of p-AgNPs or $AgNO_3$ and Glc in the medium (Pre-biofilm formation); (ii) the biofilm was allowed to form and only after that, p-AgNP or $AgNO_3$ were added (Post-biofilm formation). The exposure time to Ag was always kept constant at 24 h. Results are summarized in Figure 4. In pre-biofilm conditions the concentration of p-AgNP at which *E. coli* PHL628 viability falls to zero (MIC value) is one order of magnitude larger compared to liquid culture conditions (500 μM compared to 31.5 μM). $AgNO_3$ showed instead a MIC of 6.5μM in pre-biofilm forming condition.

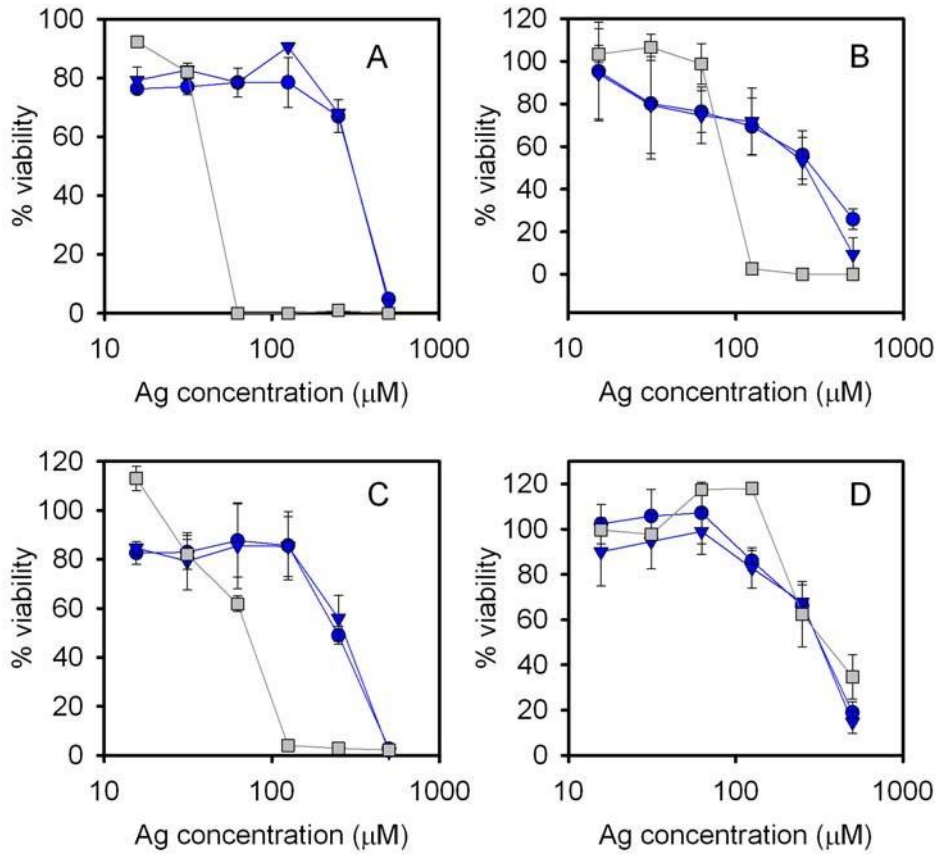

Figure 4. Viability determination as a function of Ag concentration for *E. coli* in pre-biofilm and post-biofilm conditions (A and C, respectively); same for *S. epidermidis* (B and D, respectively). Blue points refer to two different experiments carried out with two distinct p-AgNP preparations. Grey points refer to experiments performed with $AgNO_3$.

It has to be mentioned that in liquid culture conditions 62.5 μM Ag^+ reduced vitality to 55%. The slight MIC reduction in pre-biofilm conditions has thus to be attributed to the simultaneous presence of Ag^+ and glucose, and may be connected to the easier cell penetration by silver ions in such conditions due to the formation of Ag^+-glucose complexes.[36,37] Concerning *S. epidermidis* RP62A (Figure 4B), a decrease in viability at the highest concentration tested of p-AgNPs (500 μM) was observed, but the concentration with no bacterial growth (MIC value) could not be determined. Higher Ag concentrations were not tested, as our limiting upper concentration was dictated by the 1000μM Ag contained in the stock p-AgNP solution. $AgNO_3$ showed a MIC of 125 μM against *S. epidermidis* RP62A when tested in pre-biofilm forming conditions. Excluding the case of Ag^+ and *E. coli*, the overall observed increase in the MIC values is expected, since biofilms are characterized by higher resistance level to any antibacterial substance.[38-40]

In post-biofilm forming conditions, a further overall increase of resistance to both p-AgNP and Ag^+ is observed as expected, due to the mechanical resistance opposed by the extracellular matrix

produced by biofilms. The p-AgNP concentration at which *E. coli* PHL628 viability is affected and reduced to zero is 500μM (Figure 4C), while for $AgNO_3$ it is 125 μM. Concerning *S. epidermidis* RP62A (Figure 4D), a decrease in viability at the highest p-AgNP concentration (500μM) was observed, but again the concentration with no bacterial growth could not be determined. This applies also to $AgNO_3$ treatment because a complete inhibition of the bacterial growth at 500μM was not determined. Also these results were expected, since *S. epidermidis* is well known to form more resistant biofilms with respect to *E. coli*.[41]

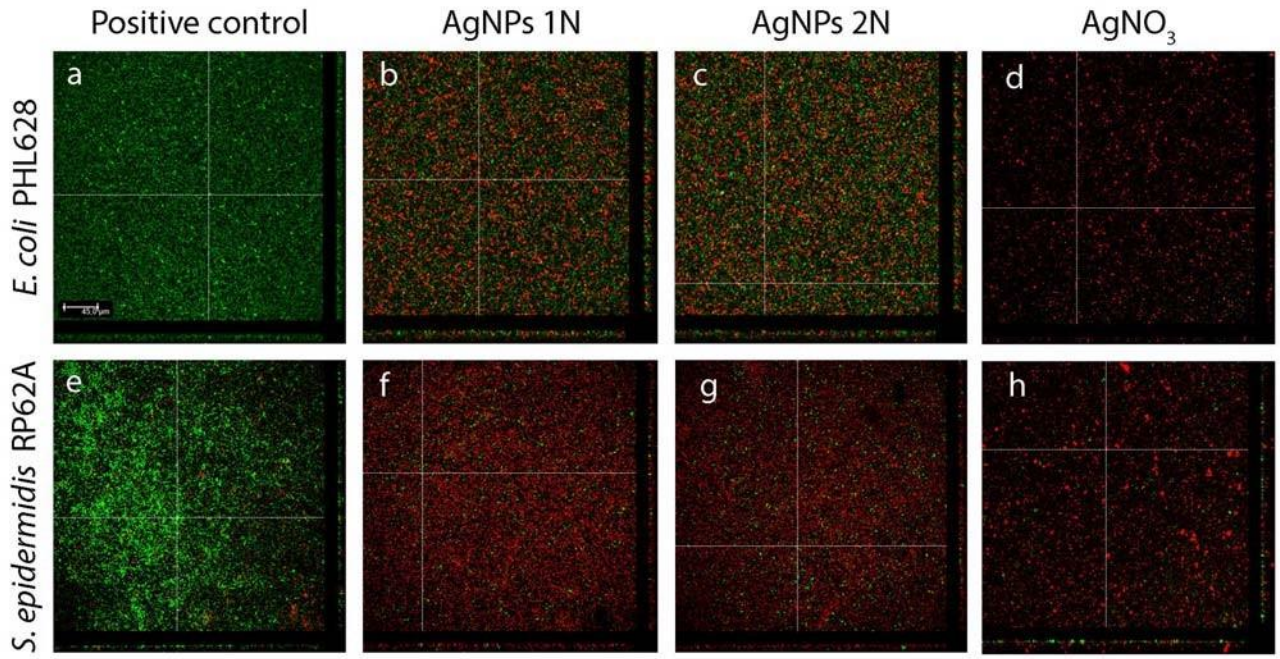

Figure 5. CLSM images of *E. coli* (**a**-**d**) and *S. epidermidis* (**e**-**f**) biofilms. Panels **a** and **e** are controls (no p-AgNP or Ag^+ treatment). Panels **b**, **c**, **f** and **g** refer to treatments with p-AgNP from two different preparations (1N panels **b** and **f**; 2N panels **c** and **g**). Panels **d** and **h** refer to treatment with ionic silver (from $AgNO_3$). Sagittal sections of the biofilms are shown below and to the right of each panel. Scale bar (see panel **a**) = 45 μm. See also SI10 for enlarged versions of the eight panels.

These data are further supported by CLSM images shown in Figure 5. Biofilms were allowed to grow for 24 h, and then incubated with either p-AgNP or Ag^+. After washing and staining, dead cells fluoresced red, while cells fluorescing green were deemed viable (see full method description in the Experimental Section). Stained biofilms were examined under CLSM, and optical sections of 0.9 μm were collected over the complete thickness of the biofilm. Figure 5 shows green-fluorescing viable cells in the control (no p-AgNP or Ag^+ added) for both bacterial strains (panels **a** and **e**). Two p-AgNP preparations (named 1N and 2N) were examined for both strains with 500 μM p-AgNP (panels **b, c, f,** and **g**) and one test was carried out with 500 μM $AgNO_3$ (panels **d** and **h**). While with ionic silver treatment almost complete cellular death was observed, and a very significant but partial reduction of viable cells was detected for both biofilms when incubated with p-AgNP.

3.4 Assessment of fibroblasts viability, cell proliferation and wound healing properties of p-AgNP.

On the basis of the low Ag^+ concentration in p-AgNP after synthesis and of the low concentration of Ag^+ released by p-AgNP when in contact with pure water through a dyalisis membrane, a good biocompatibility of such preparation was expected. We used NHDF fibroblasts to assess this. Cells were seeded on a 96-well plate, left in incubator for 24 h and then treated with p-AgNP (obtained from 0.001 M Ag at 60 °C in 1.0% pectin). In addition, we carried out the same experiment with 1.0% aqueous pectin solution as a comparison. After further 24h incubation the number of vital cells was determined and expressed as % with respect to incubation in medium without fetal bovine serum (M), to which 100% valued was assigned, and in complete medium (CM), i.e. including fetal bovine serum. Results are graphically summarized in SI11. First, cells treated with CM showed a higher percent viability with respect to those treated with M, this indicating the discriminating capability of the test. In the case of p-AgNP and of pectin solution, dilution to 1:10, 1:20 and 1:40 were used with respect to the starting material. Independently of the dilution, no cytotoxic effect was observed in both cases. On the contrary, when using p-AgNP per cent viability values were higher (120-140%) with respect to the 100% for M and to the 105-110% observed for pure pectin solutions, with values comparable to that observed for CM. Since all the samples tested were diluted in M, the obtained results indicate that the presence of p-AgNP in pectin solution improve cell viability.

SI11 graphically reports also the per cent proliferation values observed for different dilutions of p-AgNP (1:10, 1:20, 1:40 v/v in M), with M used as reference for 100%. In these experiments cells were immediately treated with p-AgNP or pure M after being seeded, then incubated for 24 h and subsequently counted. In this case, more diluted p-AgNP are more effective in promoting fibroblast proliferation, as 120% and 130 % proliferation are found for 1:20 and 1:40 dilutions, respectively. 1:10 dilution leads instead to a proliferation slightly lower than the reference (95%). This prompted us to investigate the wound healing ability of p-AgNP with an in-vitro test.[42] This is based on a method in which an insert is enclosed in a Petri dish. The insert is made of two chambers with a given area for growth (0.22 cm^2), divided by a septum that mimics the lesion area, allowing a cell-free gap of 500 (±50) μm. After fibroblast growth to confluence the insert is removed yielding two areas of cells divided by the prefixed gap, as in Figure 6A.

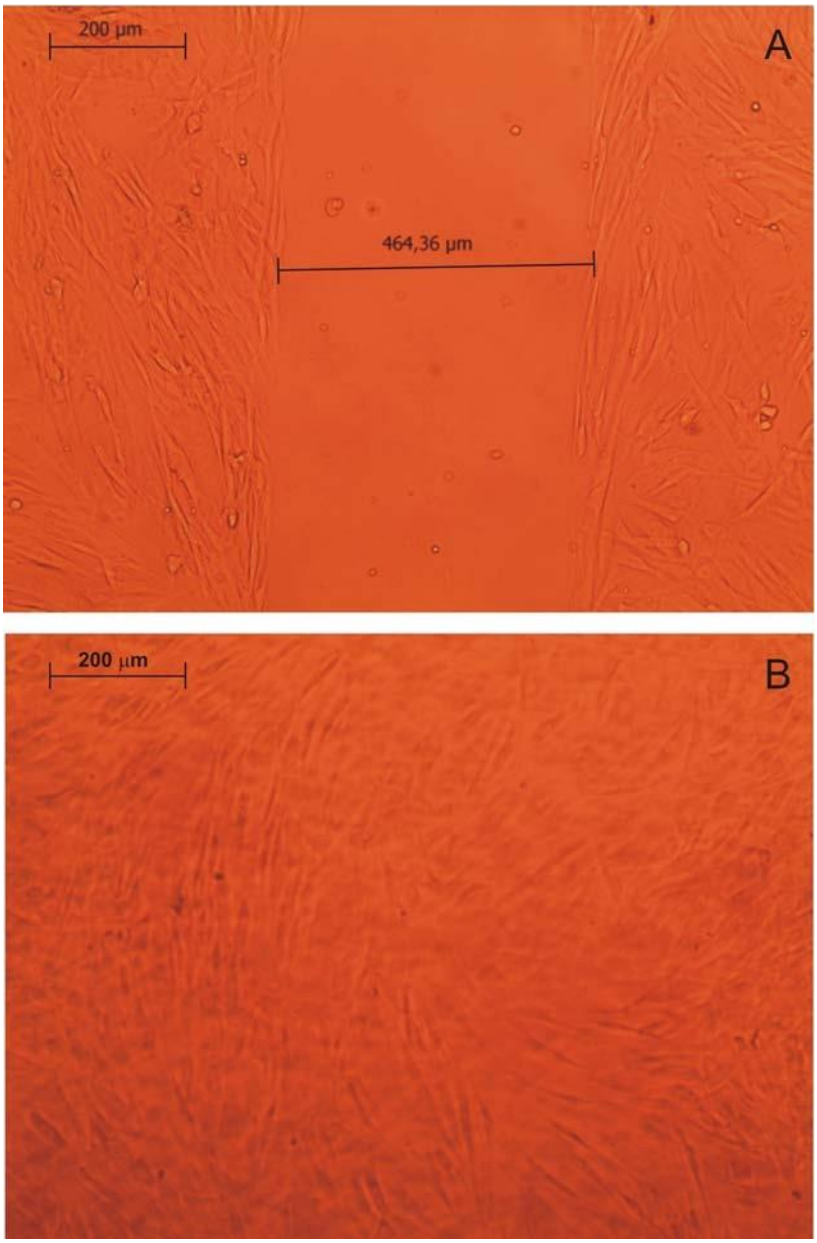

Figure 6. **A**: microphotographs of cells substrates taken at time 0, showing full, starting gap. **B**: after 72 h contact time with p AgNP

In our test, cells were then put in contact with 400 µL of 1:20 p-AgNP, a dilution chosen on the basis of the viability and proliferation results. At given times (24, 48 and 72 h) microphotograph were taken to evaluate the invasion and cell growth in the gap. Table 3 reports gap width for different contact times of p-AgNP suspension, M and CM. After 24 h
contact, no sample produced the complete closing of gap. However, it could be observed a significant ($p<0.05$) decrease of gap width for CM and p-AgNP suspension with respect to time 0, attributable to an initial invasion of cells. After 48 h, a further significant ($p<0.05$) decrease of cell width was evident for CM and p-AgNP suspension. After 72 h, the complete closing of gap is observed for CM and p-AgNP treatment, see Figure 6B, while the presence of a gap persisted for M.

	0 h	24 h	48 h	72 h
CM	464 ± 11.5 a	212 ± 34.9 b	128 ± 54.9 c	gap closed
M	539 ± 4.5 a’	532 ± 1.6 b’	496 ± 25.6 c’	469 ± 77.8d’
p-AgNP	503 ± 5.98 a’’	424 ± 28.8 b’’	239 ± 17.5 c’’	gap closed

Table 3. Width (μm) of cell gap measured after contact with samples for different time intervals (mean values ± s.d.; n=3). Anova one way-Multiple Range Test ($p<0.05$): a vs b/c/a’; b vs c/b’/b’’; c vs c’/c’’; a’ vs d’; b’ vs b/b’’; c’ vs c/c’’; a’’ vs b’’/c’’; b’’ vs b/b’/c’’; c’’ vs c/c’

Silver nanoparticles (citrate-coated) has already been shown to promote wound healing on animal models (mice) in which both thermal injuries or skin excision was carried out.[18,10] In such cases not only an antibacterial protective effect was played on the studied wounds, but also a cytokine regulatory role was observed. In our sterile model for wound healing studies the antibacterial properties of p-AgNP are of course not playing any role. However, we found here that a healing effect holds even on fibroblast colonies, that may as well be caused by cytokine regulation due to p-AgNP. It has to be stressed that both in our case and in the case of ref 10 AgNP are coated by polycarboxylates, i.e. ligands with oxygen atoms weakly interacting with the Ag surface. The favourable role played by weak O-interacting molecules, is further supported by related in-vitro increase of fibroblasts viability, that was reported for AgNP coated with glucose and lactose.[43]

4. CONCLUSIONS

A green synthesis for AgNP was investigated and optimized, in which both the reductant and the protective coating are the same natural product, i.e. pectin from citrus. Under the found optimal conditions (water, 1.0% w/w pectin, 0.001M $AgNO_3$, 60 °C for 6 h, 0.025 M OH^-) such synthesis brings multiple advantages: i) short synthesis time (6 h) with a straightforward procedure; ii) ~ 100% $Ag^+ \rightarrow Ag(0)$ conversion, with a very low

concentration of the Ag^+ cation in the product (<1 ppm); iii) excellent reproducibility and stability of the product (>> 2 weeks). Moreover, single-shape (spherical) AgNP are obtained, with a narrow dimensional distribution (d = 8.0 ±2.6 nm). The antibacterial activity and the wound healing ability of silver nanoparticles are apparently two irreconcilable properties, as the former is usually reported to require a high, sustained Ag^+ release while the latter requires low Ag^+ concentration, due to the toxicity of this cation for eukaryotic cells.[13,14] We found that p-AgNP represents an excellent compromise between these two opposite requirements. Despite the low free Ag^+ concentration, such small quantity of silver cation plus the mechanical action of AgNP allowed by the weakly interacting

pectin coating and the favourable role played by pectin adhesion to bacteria membranes combine to impart excellent antibacterial and antibiofilm properties to p-AgNP. We tested this on biofilm-forming *E. coli* (Gram-) and *S. epidermidi*s (Gram+) and on these two strains, p-AgNP antibacterial properties are comparable or superior to those of ionic Ag^+, both against planktonic cells and either on forming or preformed biofilms. In addition, not only p-AgNP demonstrated to be non-cytotoxic for fibroblasts, but also revealed capable of promoting fibroblasts proliferation and wound healing on model cultures.

All this candidate p-AgNP as an efficient green medication for repairing wounds and/or to treat the vulnerable surgical site tissues. Combating the infections acquired during surgery is the most important target in preventing implants failure. Owing to the increasing antibioticresistance in biofilm-forming bacteria that cause implant-infections, particularly early infections, antibiotic prophylaxis and therapy turn out frequently ineffective. In this connection, as resistance to silver has been rarely seen, local pre-treatment of implants with p-AgNP may be imagined as an additional, effective prophylaxis in implant surgery.

5. ACKNOWLEDGMENTS

University of Pavia (Fondo Ricerca Giovani) and CIRCMSB (Consorzio Interuniversitario di Ricerca in Chimica dei Metalli nei Sistemi Biologici) are gratefully acknowledged for support. LV would also like to thank COST Action iPROMEDAI TD1305, “Improved Protection of Medical Devices Against Infection (IPROMEDAI)” (2013-2018) (http://www.cost.eu/COST_Actions/tdp/TD1305). We are grateful to P. Vaghi (Centro Grandi Strumenti di Pavia, University of Pavia, http://cgs.unipv.it/) for technical assistance in the confocal laser scanning microscopic studies. CRA would like to acknowledge financial support from “5 per mille” contribution for Health Research to the Rizzoli Orthopaedic Institute of Bologna

References

1 T. M. Thabet, M. Tolaymat, A. M. El Badawy, A. Genaidy, K. G. Scheckel, T. P. Luxton and M. Suidan, Sci. Total Environ. 408 (2010) 999-1006.
2 B. Wiley, Y. Sun and Y. Xia, Acc. Chem. Res., 40 (2007) 1067–1076.
3 N. V. Ivanova, N. N. Trofimova and V. A. Babkin, Chem. Nat. Compd. 50 (2014) 60-64.
4 V. Kumar and S. Kumar Yadav, J. Chem. Technol. Biotechnol., 84 (2009) 151–157.
5 S. Iravani, Green Chem. 13 (2011) 2638.
6 V. K. Sharma, R. A. Yngard and Y. Lin, Adv. Colloid Interface Sci.145 (2009) 83–96.
7 E. Amato, Y. A. Diaz-Fernandez, A. Taglietti, P. Pallavicini, L. Pasotti, L. Cucca, C. Milanese, P. Grisoli, C. Dacarro, J. M. Fernandez-Hechavarria and V. Necchi, Langmuir 27 (2011) 9165–9173.

8 P. Pallavicini, A. Taglietti, G. Dacarro, Y. A. Diaz-Fernandez, M. Galli, P. Grisoli, M. Patrini, G. Santucci De Magistris and R. Zanoni, J. Colloid Interface Sci. 350 (2010) 110–116.
9 G. Nam, S. Rangasamy, B. Purushothaman and J. M. Song, Nanomater. Nanotechnol. 5 (2015) 23.
10 J. Tian, K. K. Y. Wong, C.-H. Ho, C.-N. Lok, W.-Y. Yu, C.-M. Che, J.-F. Chiu and P. K. H. Tam., ChemMedChem 2 (2007), 129 – 136.
11 Rigo C., Ferroni L., Tocco I., Roman M., Munivrana I., Gardin C., Cairns W.R.L., Vindigni V., Azzena B., Barbante C., Zavan B. Int. J. Mol. Sci. 14 (2013) 4817–4840
12 Liu X., Lee P.Y., Ho C.M., Lui V.C., Chen Y., Che C.M., Tam P.K., Wong K.K., Chem. Med.Chem. 5 (2010) 468–475
13 S. Chernousova and M. Epple, Angew. Chem. Int. Ed., 52 (2013) 1636 – 1653.
14 A. Milheiro, K. Nozaki, C. J. Kleverlaan, J. Muris, H. Miura and A. J. Feilzer, Odontology, 104 (2016) 136–142.
15 Arciola C.R., Campoccia D., Speziale P., Montanaro L., Costerton J.W. Biomaterials 33 (2012) 5967-5982
16 A. Taglietti, Y. A. Diaz Fernandez, E. Amato, L. Cucca, G. Dacarro, P. Grisoli, V. Necchi, P. Pallavicini, L. Pasotti and M. Patrini, Langmuir 28 (2012) 8140−8148 17 Z. K. Mukhiddinov, D. Kh. Khalikov, F. T. Abdusamiev, Ch. Ch. Avloev, Talanta, 53 (2000) 171–176.
18 B. R. Thakur, R. K. Singh and A. K. Handa, Crit. Rev. Food Sci. Nutr. 37 (1997) 47– 73.
19 I. G. Plaschina, E. E. Braudo and V. B. Tolstoguzov, Carbohyd. Res., 60 (1978) 1-8.
20 D. Asker, J. Weiss and D. J. McClements, Langmuir 25 (2009) 116–122.
21 Zahran M.K., Ahmed H.B., El-Rafie M.H. Carbohyd. Polym. 111 (2014) 971–978
22 M.K.A. Al-Muhanna, K.S. Hileuskaya, V.I. Kulikouskaya, A.N. Kraskouski, V.E. Agabekov, Colloid J+, 77 (2015) 677–684
23 K. Songsilawat, J. Shiowatana and A. Siripinyanond, J. Chromatogr. A 1218 (2011) 4213–4218.
24 K. Nigoghossian, M. V. dos Santos, H. S. Barud, R. R. da Silva, L. A. Rocha, J. M. A. Caiut, R. M. N. de Assunção, L. Spanhel, M. Poulain, Y. Messaddeq, S. J. L. Ribeiro, Appl. Surf. Sci. 341 (2015) 28–36.
25 D. Arora, N. Sharma, V. Sharma, V. Abrol, V. Shankar, S. Jaglan, Appl. Microbiol. Biotechnol. 100 (2016) 2603–2615.
26 N. V. Ivanova, N. N. Trofimova, V. A. Babkin, Chem. Nat. Compd. 50 (2016) 60-64.
27 R. Kataky, M. R. Bryce, B. Johnston, Analyst 125 (2000) 1447–1451.
28 A. Cochis, B. Azzimonti, R. Sorrentino, C. Della Valle, E. De Giglio, N. Bloise, L. Visai, G. Bruni, S. Cometa, D. Pezzoli, G. Candiani, L. Rimondini, R. Chiesa, Data Brief, 6 (2016) 758-762
29 S. Ravishankar, D. Jaroni, L. Zhu, C. Olsen, T. McHugh, M. Friedman, J. Food Sci. 77 (2012) M377-M382.
30 G. C. Jayakumar, N. Usharani, K. Kawakami, J. R. Rao, B. U. Nair, RSC Adv. 4 (2014) 42846–42854.
31 Q. L. Feng, J. Wu, G. Q. Chen, F. Z. Cui, T. N. Kim, J. O. Kim., J. Biomed. Mater. Res. 52 (2000) 662–668.
32 K. J. Woo, H. C. Koo, K. W. Kim, S. Shin, S. H. Kim and Y. H. Park, Appl. Environ. Microbiol. 74 (2008) 2171–2178.
33 Y. Xiong, M. Brunson, J. Huh, A. Huang, A. Coster, K. Wendt, J. Fay, D. Qin, Small 9 (2013) 2628–2638.
34 G. A. Martínez-Castañón, N. Niño-Martínez, F. Martínez-Gutierrez, J. R. MartínezMendoza, F. Ruiz, J. Nanopart. Res. 10 (2008) 1343-1348.
35 S. W. Kim, Y.-W. Baek and Y. J. An, Appl. Microbiol. Biotechnol. 92 (2011) 1045– 1052.

36 A. Baksi, M. Gandi, S. Chaudhari, S. Bag, S. S. Gupta and T. Pradeep, Angew. Chem. Int. Ed. 55 (2016) 7777–7781.
37 L. Boutreau, E. Leon, J.-Y. Salpin, B. Amekraz, C. Moulin, J. Tortajada, Eur. J. Mass Spectrom. 9 (2003) 377–390.
38 L. Hall-Stoodley, J. W. Costerton, P. Stoodley, Nature Rev. Microbiol., 2 (2004) 95108.
39 R. Y. Pelgrift, A. J. Friedman, Adv. Drug Delivery Rev. 65 (2013) 1803–1815.
40 P. S. Stewart, J. W. Costerton, Lancet 358 (2001) 135–38.
41 R. M. Donlan and J. W. Costerton, Clinical Microbiology Reviews 15 (2002) 167-193.
42 M. Mori, S. Rossi, M. C. Bonferoni, F. Ferrari, G. Sandri, F. Riva, C. Del Fante, C. Perotti, C. Caramella, Int. J. Pharm. 461 (2014) 505- 513.
43 I. Sur, D. Cam, M. Kahraman, A. Baysal, M. Culha, Nanotechnology 21 (2010) 175104.

FIGURE CAPTIONS

Figure 1 Working and reaction scheme for pectin/Ag^+ reaction at basic pH. The blue circles in the lower sketch represent alcoholic and aldehyde functions, red circles represent carboxylates

Figure 2. **A** and **C**: series of absorption spectra in a solution of 1% pectin/Ag^+ at basic pH, at 20 °C (panel A) and at 60 °C (panel C); the time at which spectra were taken can be read by the color in the inset list. **B** and **D**: absorbance at the LSPR maximum (411 nm) vs time, obtained from the spectra of panel A and C, respectively. **E**: TEM image obtained from a preparation with 1% pectin/Ag^+, 60 °C

Figure 3. IR spectra. **A**: pectin as such, black; pectin after treatment at pH 12, 50 °C, red. **B**: p-AgNP product under standard synthetic conditions (Ag^+ 0.001 M, 1.0% pectin, 60°C), blue); same, but with excess Ag^+ (equimolar with galacturonic acid units), green. The wavenumber of the relevant bands are reported in the figure

Figure 4. Viability determination as a function of Ag concentration for *E. coli* in pre-biofilm and post-biofilm conditions (A and C, respectively); same for *S. epidermidis* (B and D, respectively). Blue points refer to two different experiments carried out with two distinct pAgNP preparations. Grey points refer to experiments performed with $AgNO_3$.

Figure 5. CLSM images of *E. coli* (**a**-**d**) and *S. epidermidis* (**e**-**f**) biofilms. Panels **a** and **e** are controls (no p-AgNP or Ag^+ treatment). Panels **b**, **c**, **f** and **g** refer to treatments with p-AgNP from two different preparations (1N panels **b** and **f**; 2N panels **c** and **g**). Panels **d** and **h** refer to treatment with ionic silver (from $AgNO_3$). Sagittal sections of the biofilms are shown below and to the right of each panel. Scale bar (see panel **a**) = 45 μm. See also SI10 for enlarged versions of the eight panels.

Figure 6. **A**: microphotographs of cells substrates taken at time 0, showing full, starting gap.
B: after 72 h contact time with p AgNP

TABLES

% pectin	AgNP diameter (nm)[a]		LSPR band, λ_{maxb}(nm)	
	20 °C	60 °C	20°C	60 °C
0.5	8.3 (3.0)	8.0 (3.6)	411(68)	409(63)
1.0	8.8 (3.5)	8.0 (2.6)	412(69)	412(63)
2.0	8.4 (3.4)	8.0 (3.6)	411(63)	416(61)

Table 1. Dimensional and optical data for p-AgNP prepared with 0.001M $AgNO_3$. [a]standard deviation in parenthesis; [b]width at half height (nm) in parenthesis

	E. coli PHL628		*S. epidermidis* RP62A	
	6h	24h	6h	24h
p-AgNP[a]	15.62 µM	31.25 µM	250 µM	500 µM
Ag^+ ($AgNO_3$)	-[b]	125 µM	-[b]	125 µM
gsh-AgNP[c]	-[b]	140 µM	-[b]	1680 µM[d]

Table 2: MIC values for p-AgNP and ionic silver in liquid culture conditions. [a]experiments were repeated two times on two different p-AgNP preparations, with identical results; [b]MIC for Ag^+ was not determined at 6h; [c]values from ref 7; [d]data obtained with *S. aureus*

	0 h	24 h	48 h	72 h
CM	464 ± 11.5 a	212 ± 34.9 b	128 ± 54.9 c	gap closed
M	539 ± 4.5 a’	532 ± 1.6 b’	496 ± 25.6 c’	469 ± 77.8d’
p-AgNP	503 ± 5.98 a’’	424 ± 28.8 b’’	239 ± 17.5 c’’	gap closed

Table 3. Width (µm) of cell gap measured after contact with samples for different time intervals (mean values ± s.d.; n=3). Anova one way-Multiple Range Test ($p<0.05$): a vs b/c/a’; b vs c/b’/b’’; c vs c’/c’’; a’ vs d’; b’ vs b/b’’; c’ vs c/c’’; a’’ vs b’’/c’’; b’’ vs b/b’/c’’; c’’ vs c/c’

SUPPORTING MATERIAL

SI – Details on experimental methods.

Ag^+ release studies. A 20 mL volume of p-AgNP prepared from 1 mM Ag^+ in 1.0% w/w pectin was cooled at room temperature after 12h at 60 °C and subsequently confined inside a dialysis membrane tube (Mires Emanuele – Milano, Molecular Weight Cut Off (MWCO) 12-14000 Dalton, 28.5 mm diameter), that was immersed in 20.0 mL bidistilled water (external liquid phase). At given times (0.5, 1, 3, 6, 24 h), 3.0 mL of the external liquid phase was collected, treated with 100 µL of 1.0 M HNO_3 and analysed with an ICP-OES Optima 3000 Perkin Elmer instrument. A volume of 3.0 mL bidistilled water was re-added after each sampling in the external liquid phase to maintain its starting volume.

Differential scanning calorimetry (DSC) and thermogravimetric analysis (TGA) were run on dry p-AgNP, prepared as described. A simultaneous thermogravimetric – calorimetric Q600 analyser by TA Instrument was used.10 mg samples were dispersed in an open alumina crucible and heaten at 10 °C/min from room temperature to 1000°C under a nitrogen flux. Pure pectin was also analysed. Before analysis it was subjected to the same experimental conditions used for p-AgNP synthesis (12 h at 60 °C in basic solution, dilution with ethanol, ultracentrifugation, drying). Thermogravimetric analysis was run with a Q5000 TA Instrument thermobalance by heating 10 mg sample in a Pt crucible under inert atmosphere, from 25 °C to 1000 °C, at a 10 °C/min rate. Thermogravimetric and calorimetric curves can be found in SI6.

X-ray diffraction was run on dry p-AgNP, prepared as described, using a Bruker D5005 instrument with Bragg-Brentano geometry. Powders were deposited on a silicon slide cut with an orientation avoiding diffraction in the used instrument geometry, and analysed from 10° to 80° with a 0.02° angular step and 10 seconds per step. An X-ray diffraction pattern is included in SI7.

TEM imaging. TEM (transmission electron microscope) images were taken on a Jeol JEM1200 EX II instrument on 10 µL samples, deposited on Nickel grids (300 mesh) covered with a Parlodion membrane.

Dynamic Light Scattering (DLS) and Z-potential. DLS experiments were carried out on a Malvern Zetasizer NanoZS90 instrument. Z-potential was measured with the same instrument using a dedicated Malvern device.

Confocal Laser Scanning Microscopy (CLSM) studies. For confocal studies, 1.5 ml of diluted bacterial suspensions were dispensed into 24-well microplates (Costar) containing on the bottom sterile glass coverslips. Coverslips containing bacterial suspensions were incubated for 24 h at 37° C to allow biofilm formation. After a delicate wash with PBS, either p-AgNPs or $AgNO_3$ (final concentration 500 µM) were added to formed biofilms. After 24 hours, the viability of bacteria within the biofilms after p-AgNPs or $AgNO_3$ treatment was estimated with the BacLight Live/Dead viability kit (Molecular Probes, Eugene, OR, USA). The kit includes two fluorescent nucleic acid stains: SYTO9 and propidium iodide. SYTO9 penetrates both viable and nonviable bacteria, while propidium iodide penetrates bacteria with damaged membranes and quenches SYTO9 fluorescence. Dead bacteria, which take up propidium iodide, fluoresce red, and bacteria fluorescing green are deemed viable. For assessing viability, 1 µl of the stock solution of each stain was added to 3 ml of PBS and, after being mixed, 500 µL of the solution was dispensed into 24-well microplates containing treated and untreated biofilms and incubated at 22° C for 15 min in the dark. Stained biofilms were examined under a Leica CLSM (model TCS SPII; Leica, Heidelberg, Germany) using a 40x oil immersion objective.

The excitation and emission wavelengths used for detecting SYTO9 were 488 and 525 nm, respectively. Propidium iodide was excited at 520 nm, and its emission was monitored at 620 nm. The optical sections of 0.9 µm were collected over the complete thickness of the biofilm, and for each sample, images from three randomly selected positions were acquired.

NHDF fibroblast cell culture. NHDF fibroblasts (juvenile fibroblast from foreskin) (Promocell GmbH, Heidelberg, Germany) from 6^{th} to 16^{th} passage were used. Cells were cultured in a polystyrene flask (Greiner bio-one, PBI International, Milan, Italy) with 13–15 ml of complete culture medium, consisting of Dulbecco's modified Eagles medium with 4.5 g/L glucose and l-glutamine supplemented with 1% Antibiotic Antimycotic Solution and 10% (v/v) inactivated foetal calf bovine serum. Cells were maintained in incubator (Shellab® Sheldon® Manufacturing Inc., Oregon, USA) at 37°C with 95% air and 5% CO_2 atmosphere. All the operations required for cell culture were carried out in a vertical laminar air flow hood (Ergosafe Space 2, PBI International, Milan, Italy). After the cells had reach 80–90% confluence in the flask (one week) a trypsinization was performed: at first, the monolayer was washed with Dulbecco's Phosphate Buffer Solution in order to remove bivalent cations that could inactivate trypsin, then 3 mL of 0.25% (w/v) trypsin-EDTA solution was left in contact with the monolayer for 5 min. After that time, the cell layer was harvested with 7 mL of the CM to stop the proteolytic activity of trypsin and to facilitate the detachment of cells. Afterwards, cell suspension was centrifuged (TC6, Sorvall Products, Newtown, USA) at 1500 rpm for 10 min. The supernatant was eliminated and then the cells were re-suspended in 6 ml of CM. The amount of cells in suspension was determined in a counting chamber (Hycor Biomedical, Garden Grove, California, USA), using 0.5% (w/v) trypan blue solution to visualize and count viable cells.

SI1 – Absorption spectra at 24h and control spectra at t ≥ 5days for Ag^+ 0.001M

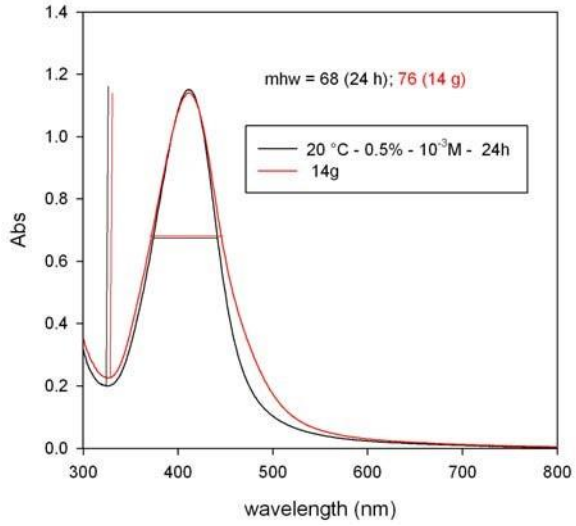

A

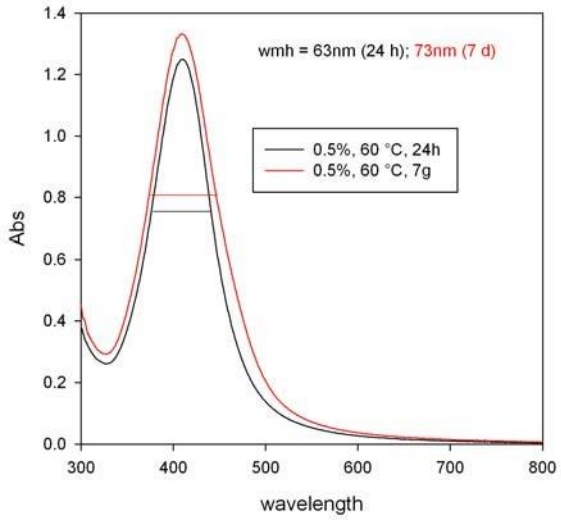

B

SI1A-B. **A**, absorption spectra for 0.5 % pectin, 0.001M Ag^+, 20 °C, 24h and 14 d. **B**, same, 60 °C, 24h and 7 d. The red and black vertical lines indicates how we calculated the width at half height (mhw, middle height width in the figures). The height is calculated from top of the peak to the maximum on the left side of the bands. This method has been used for all spectra in this paper, so that the mhw values can be compared.

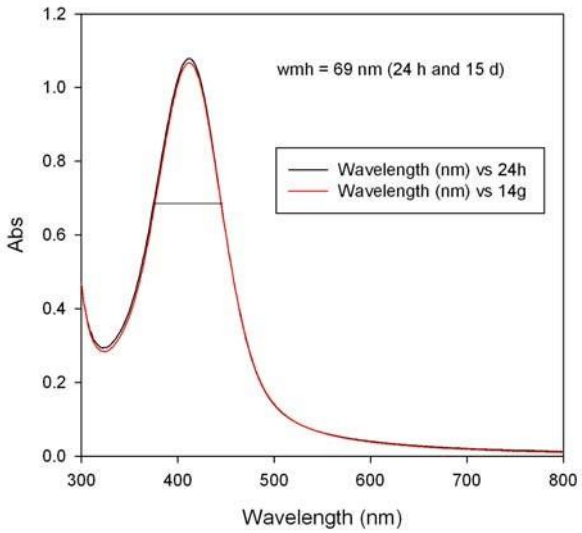

C

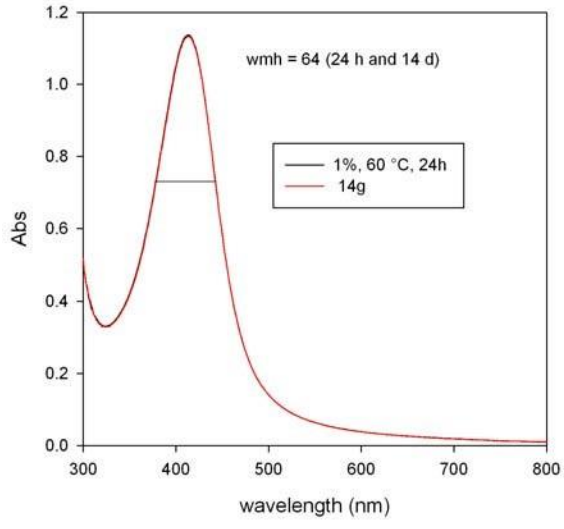

D

SI1C-D. **C**, absorption spectra for 1.0 % pectin, 0.001M Ag^+, 20 °C, 24h and 14 d. **D**, same, 60 °C, 24h and 14 d.

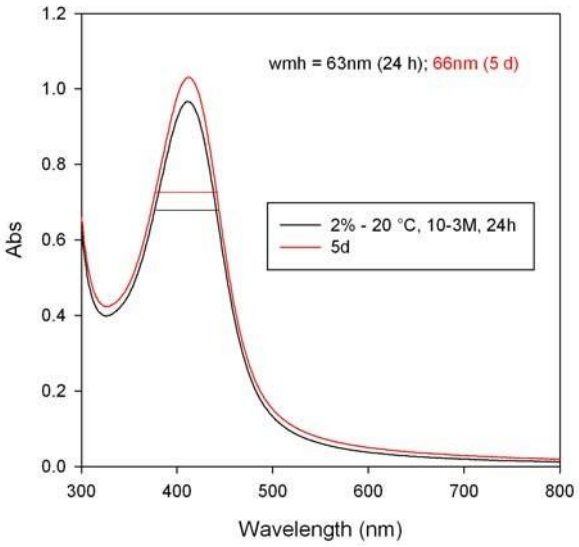

E

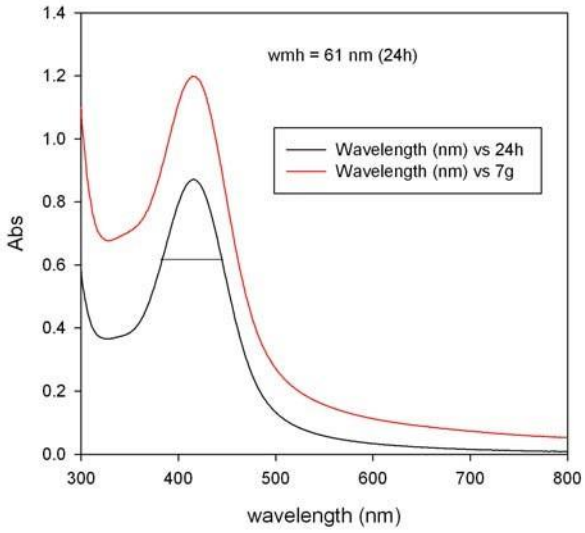

F

SI1E-F. **E** absorption spectra for 2.0 % pectin, 0.001M Ag^{+}, 20 °C, 24h and 5 d. **F**, same, 60 °C, 24h and 7d

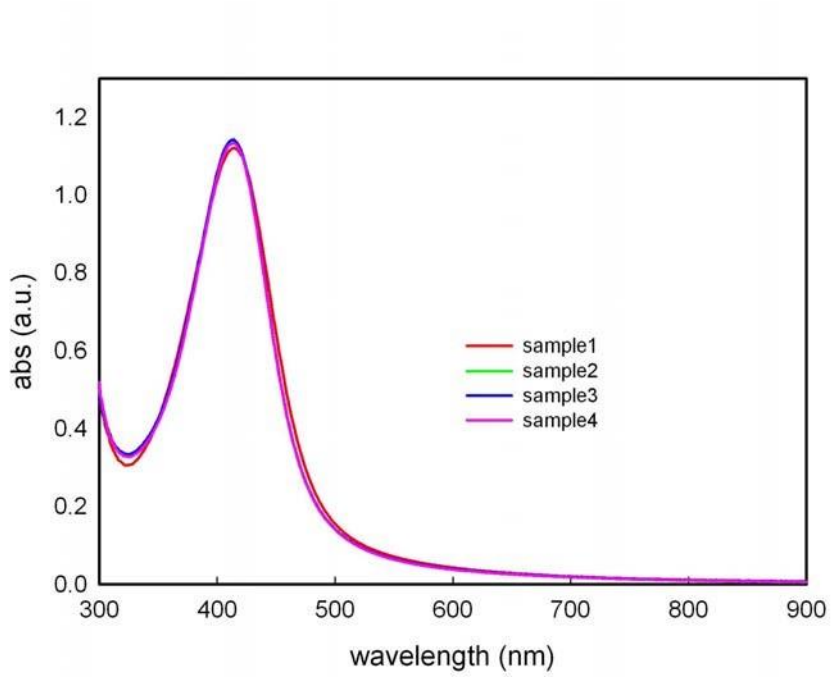

SI1G. Absorption spectra from 4 different preparation with 0.001Ag^{+}, 1.0% pectin, 60 °C (24 h time).

SI2 TEM images and dimensional determination for Ag^{+} 0.001M

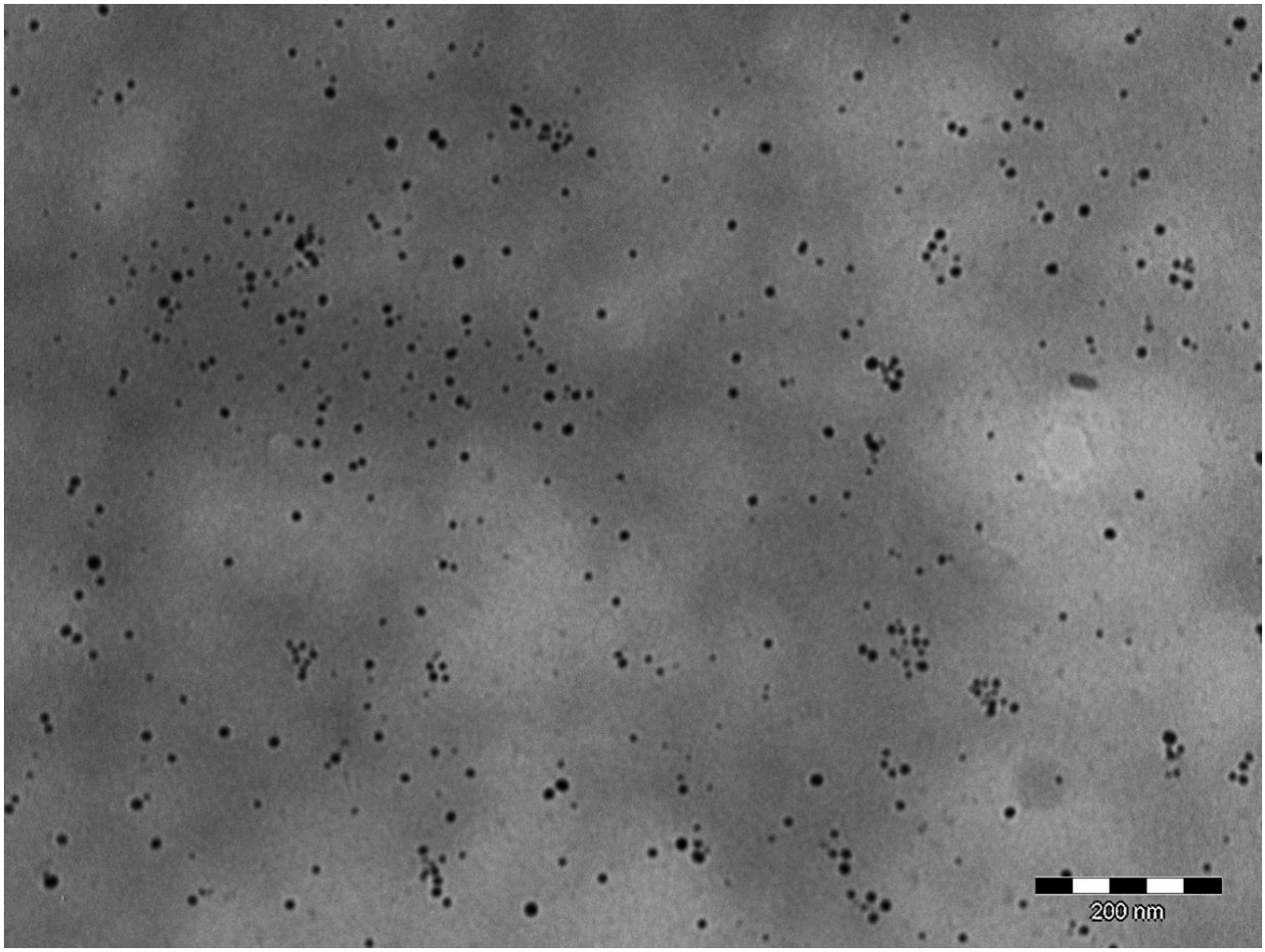

SI2A. Example of TEM image for a 0.001M Ag^{+}, 1% pectin, 60 °C synthesis

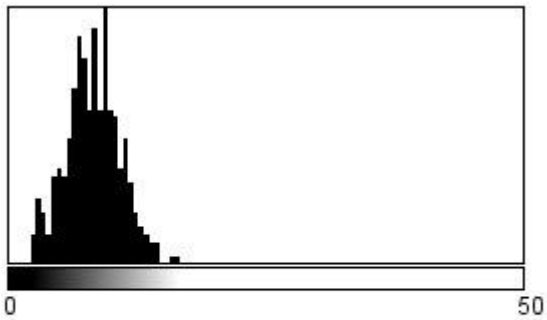

SI2B. Dimensional counting from the same image

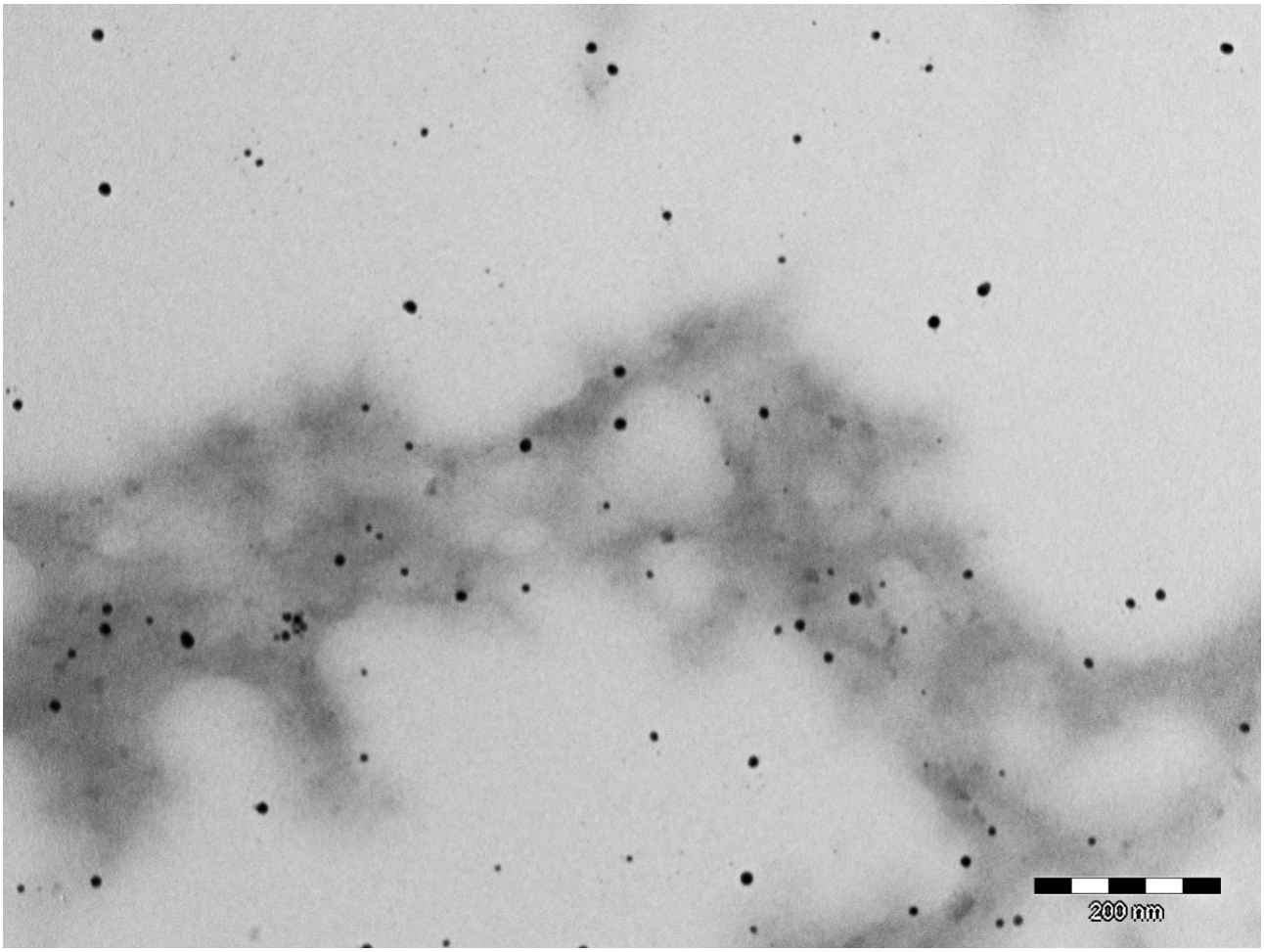

SI2C. Example of TEM image for a 0.001M Ag^{+}, 0.5% pectin, 20 °C synthesis

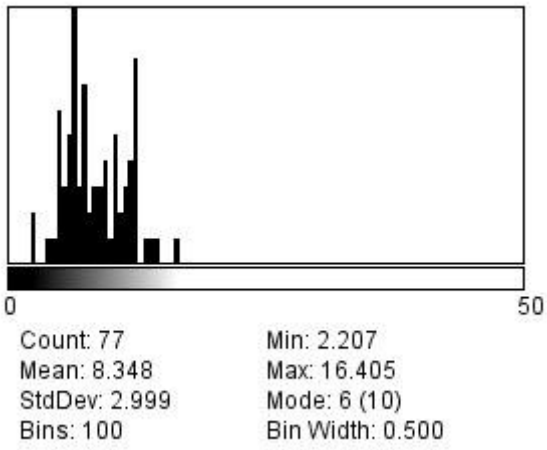

SI2D. Dimensional counting from the same image

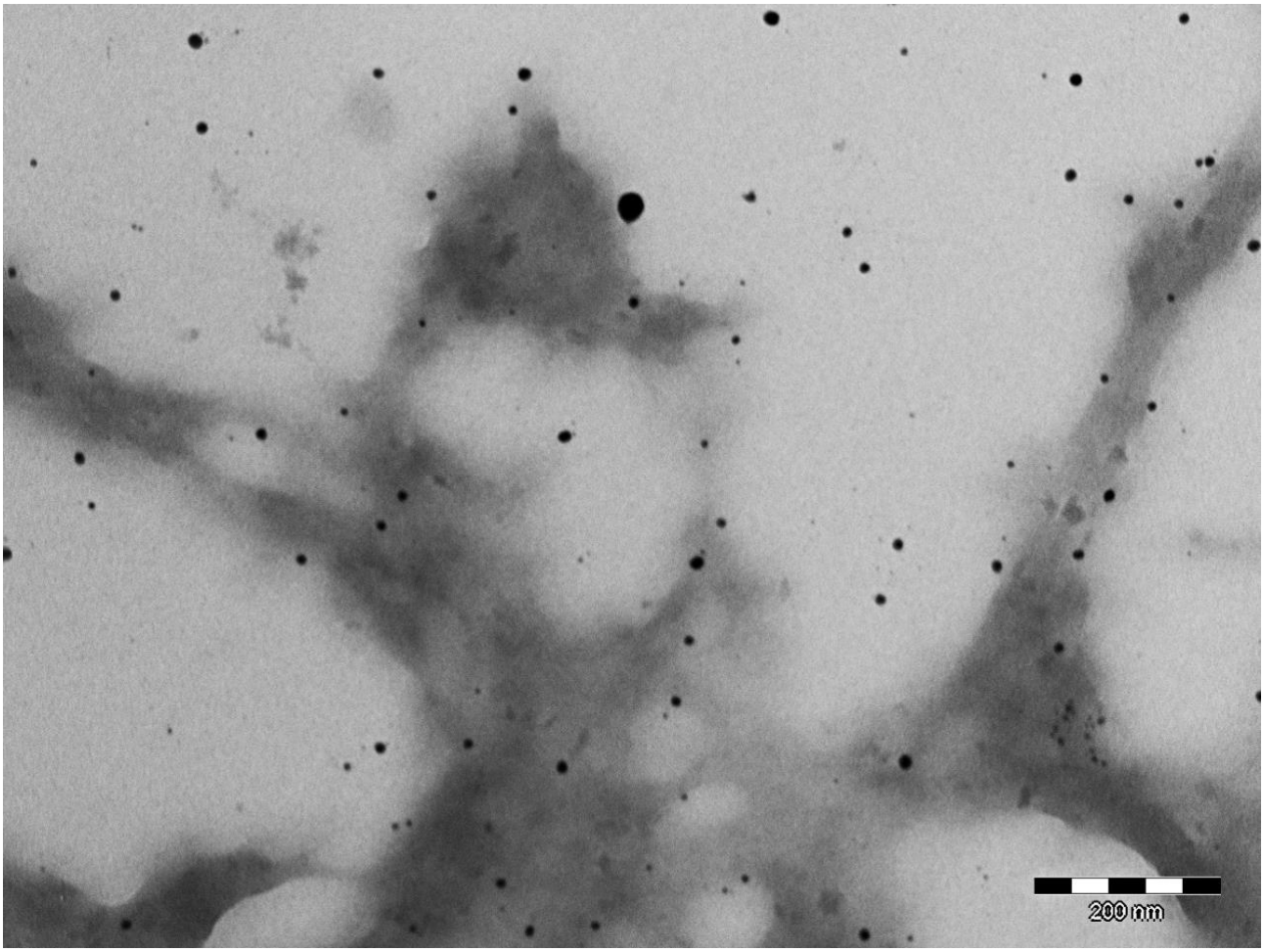

SI2E. Example of TEM image for a 0.001M Ag^{+}, 0.5% pectin, 60 °C synthesis

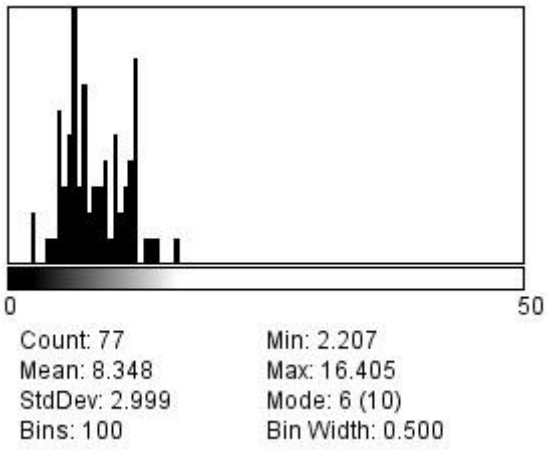

SI2F. Dimensional counting from the same image

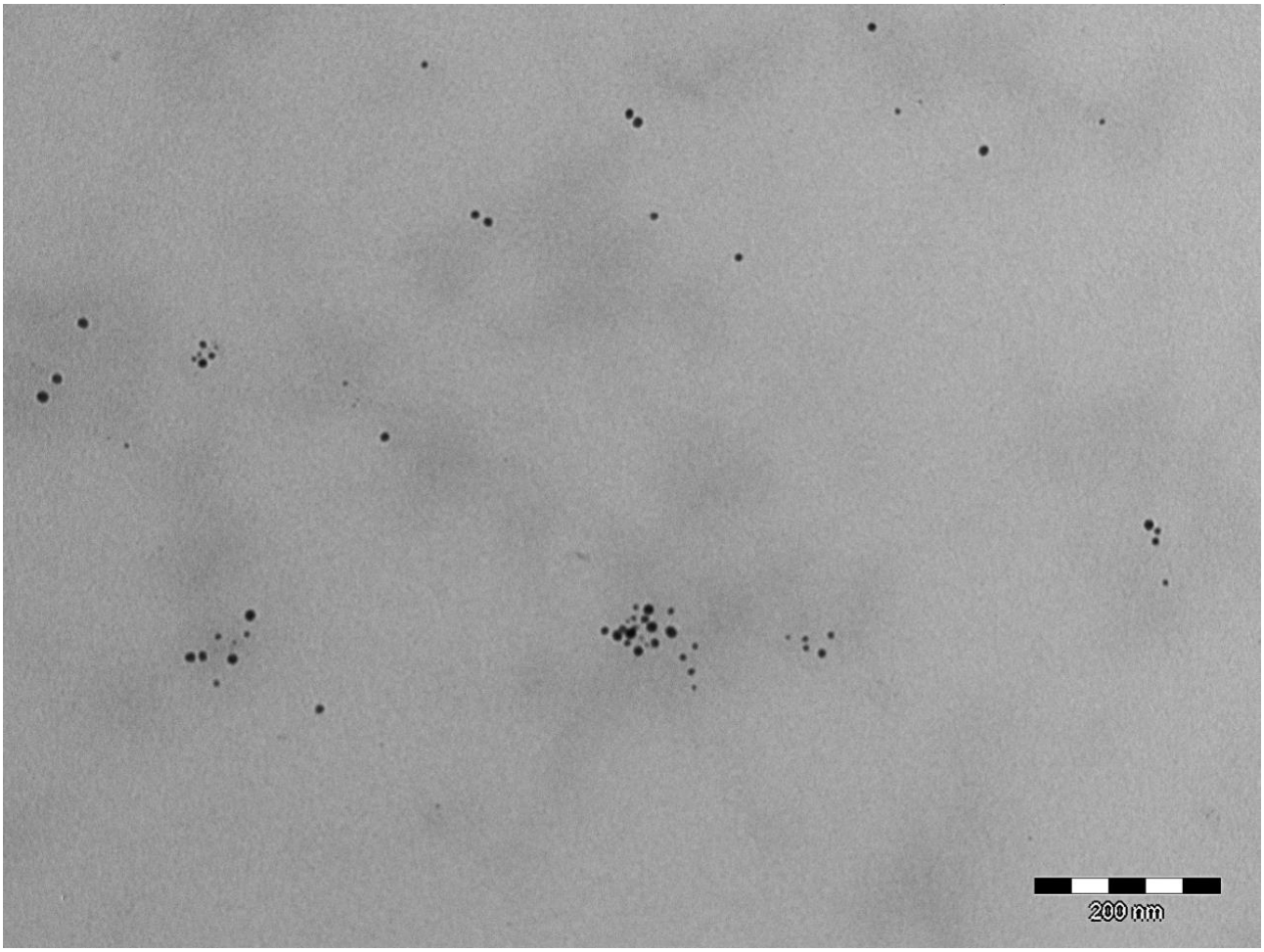

SI2G. Example of TEM image for a 0.001M Ag^+, 2% pectin, 60 °C synthesis

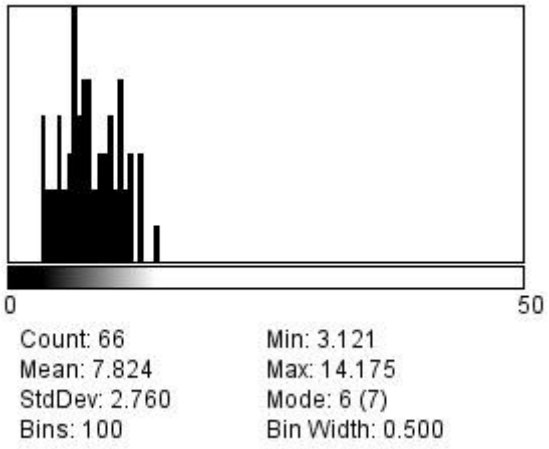

SI2H. Dimensional counting from the same image

SI3 – Absorption spectra for syntheses with Ag^+ 0.01M

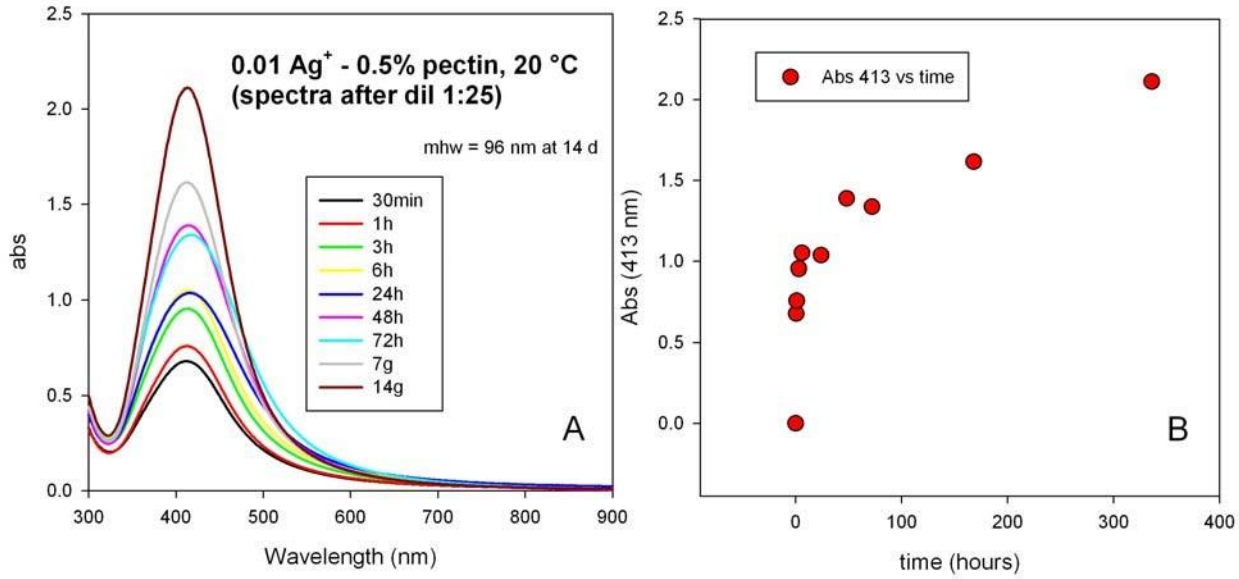

FigureSI3A-B. **A**: series of absorption spectra for 0.01Ag^{+} in 0.5% pectin at 20 °C (from 30 min to 14 days). **B**: absorption at λmax (413 nm) vs time (data taken from Figure SI3A).

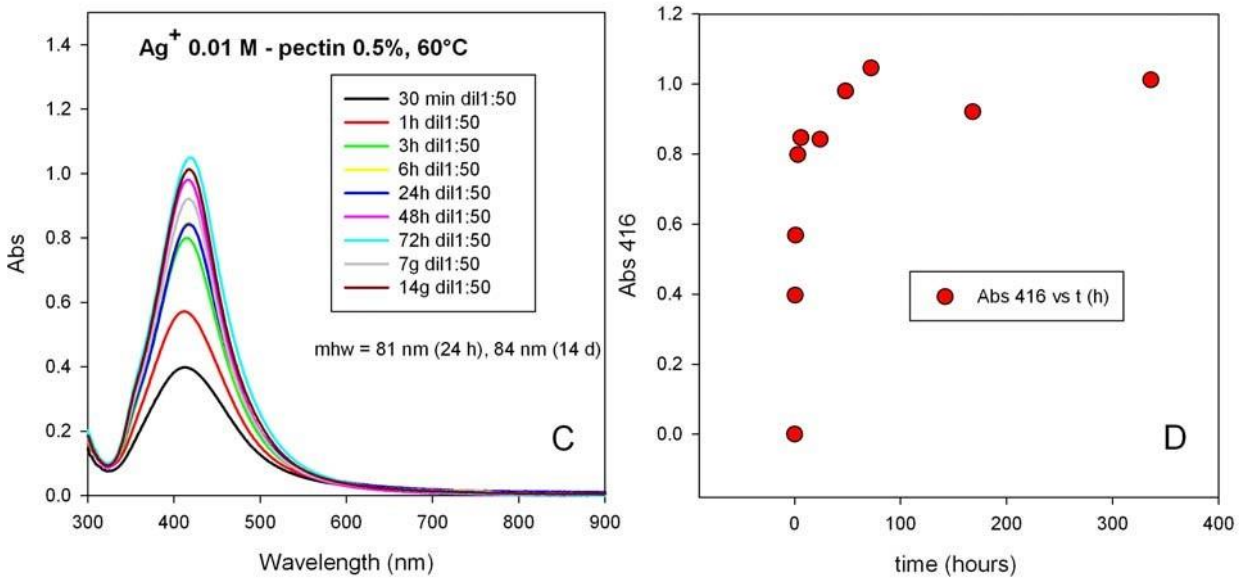

FigureSI3C-D. **C**: series of absorption spectra for 0.01Ag^{+} in 0.5% pectin at 60 °C (from 30 min to 14 days). **D**: absorption at λmax (416 nm) vs time (data taken from Figure SI3C).

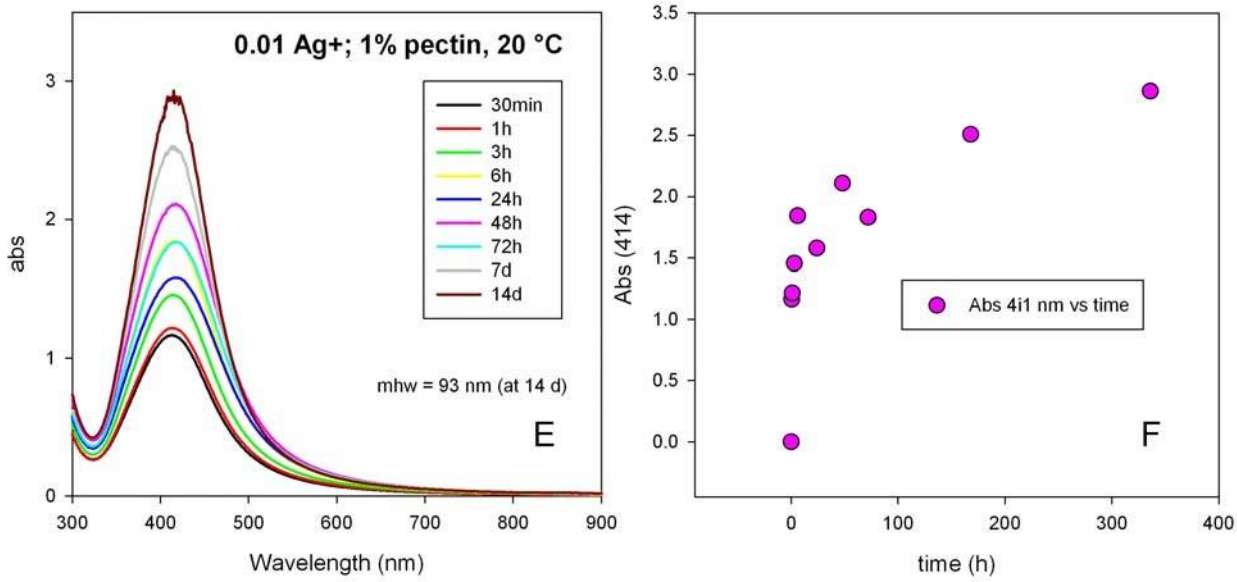

FigureSI3E-F. **E**: series of absorption spectra for 0.01Ag^{+} in 1% pectin at 20 °C (from 30 min to 14 days). **F**: absorption at λmax (414 nm) vs time (data taken from Figure SI3E).

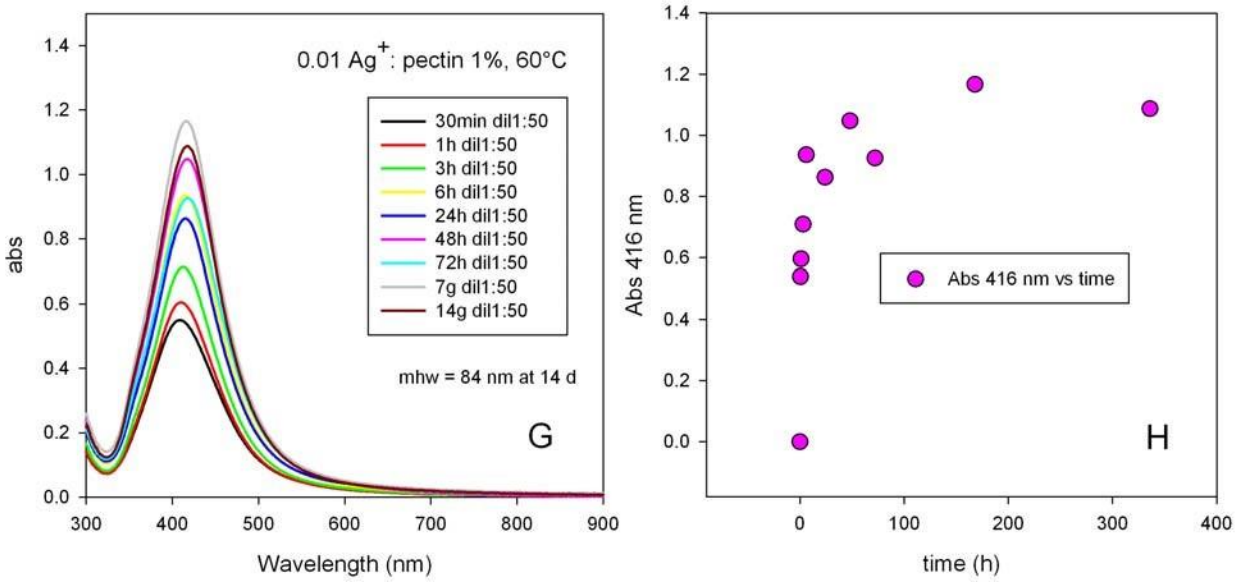

FigureSI3G-H. **G**: series of absorption spectra for 0.01Ag in 1% pectin at 60 °C (from 30 min to 14 days). **H**: absorption at λmax (416 nm) vs time (data taken from Figure SI3G).

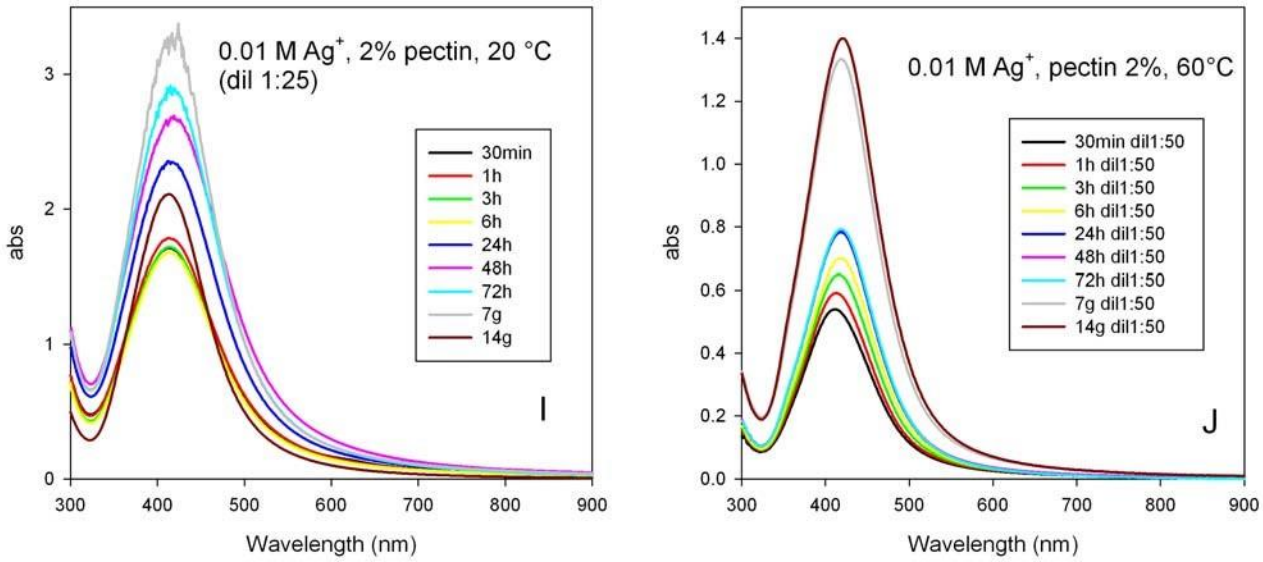

Figure SI3I-J. Series of spectra for 0.01M Ag+ in 2% pectin at 20 °C (**I**) and 60 °C (**J**). Time 30 min-14 days

SI4 – TEM images for syntheses with 0.01 M Ag^+

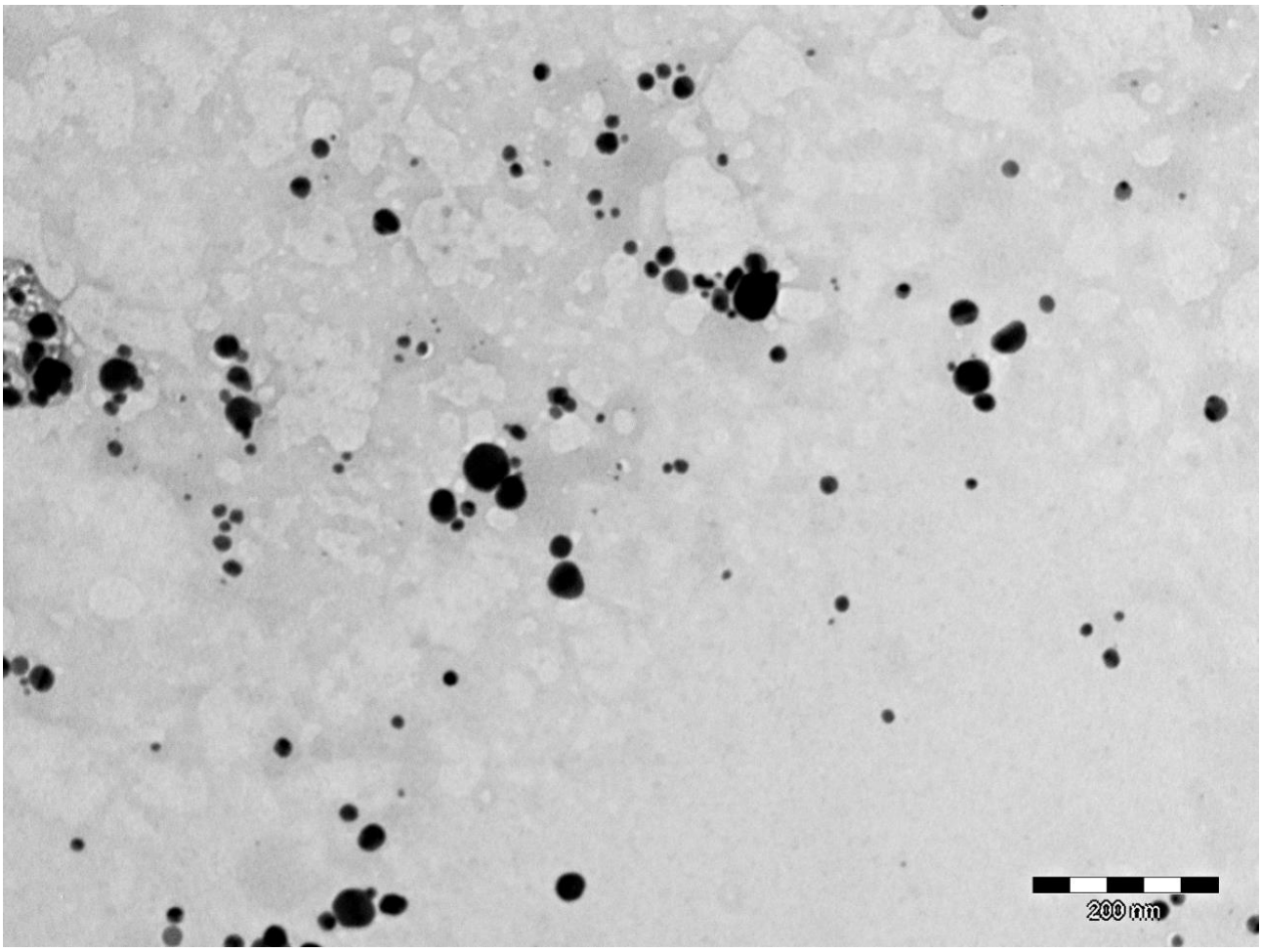

Figure SI4A: TEM image for synthesis with 0.01M Ag^+, 0.5% pectin, 60 °C

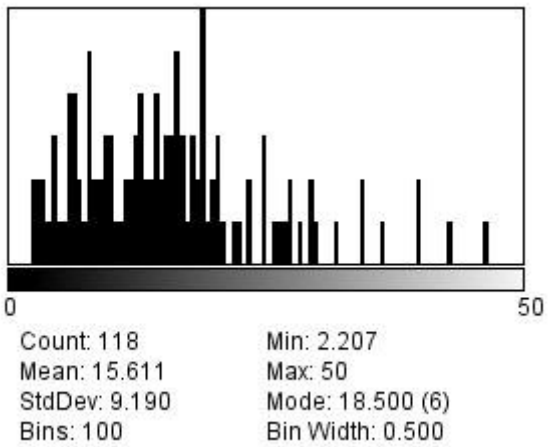

Figure SI4B: dimensional counting from the previous image

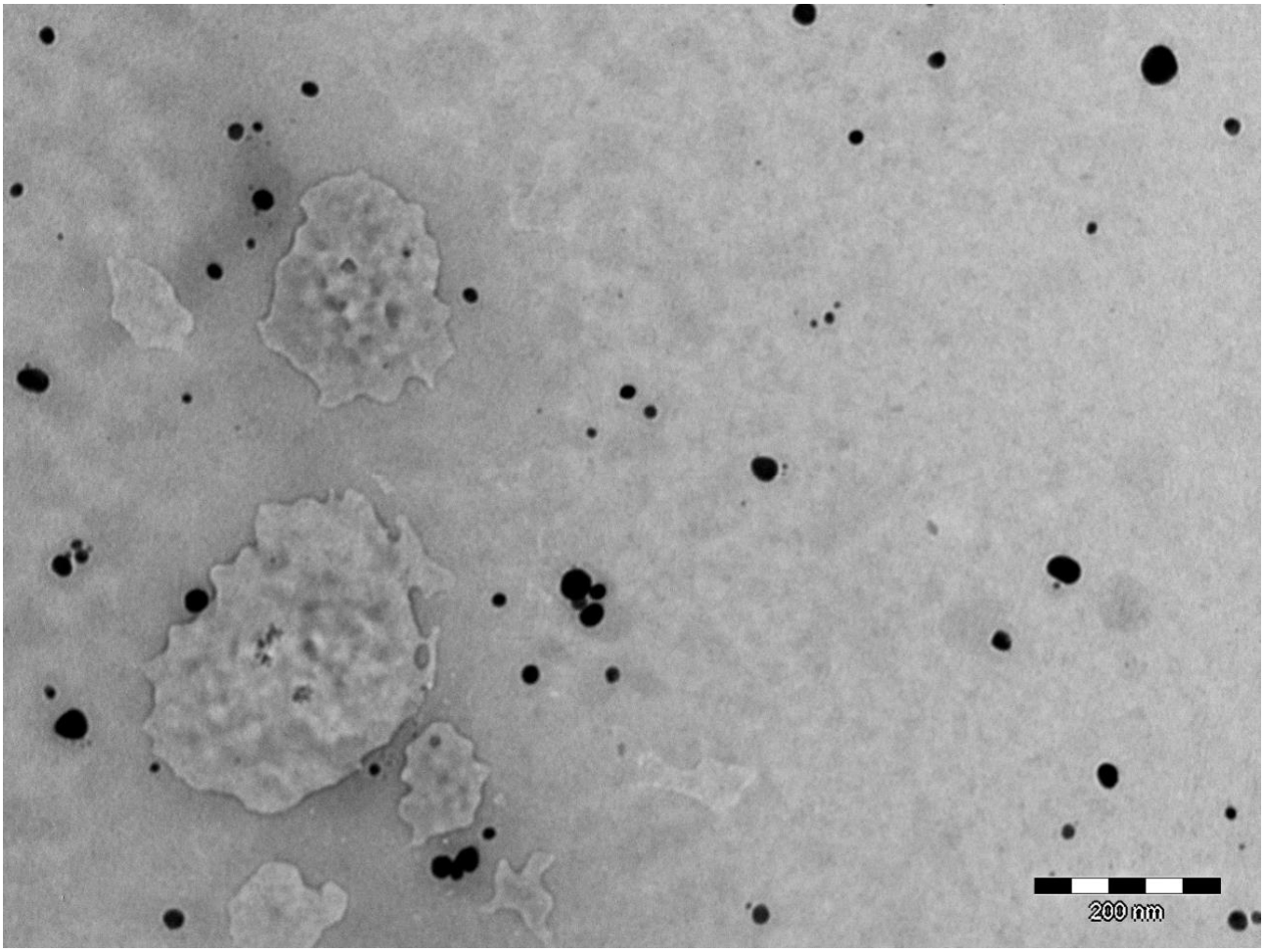

Figure SI4C: TEM image for synthesis with 0.01M Ag^{+}, 1.0% pectin, 60 °C

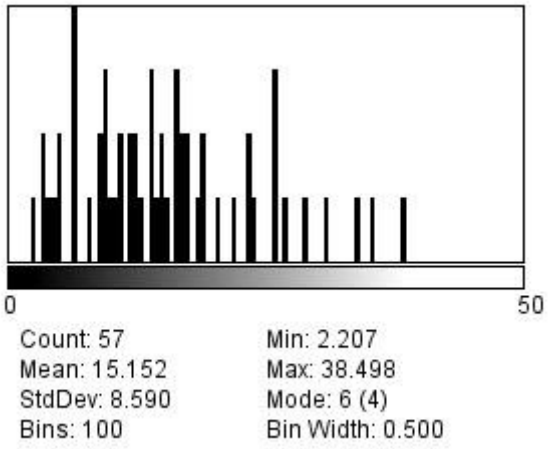

Figure SI4D: dimensional counting from the previous image

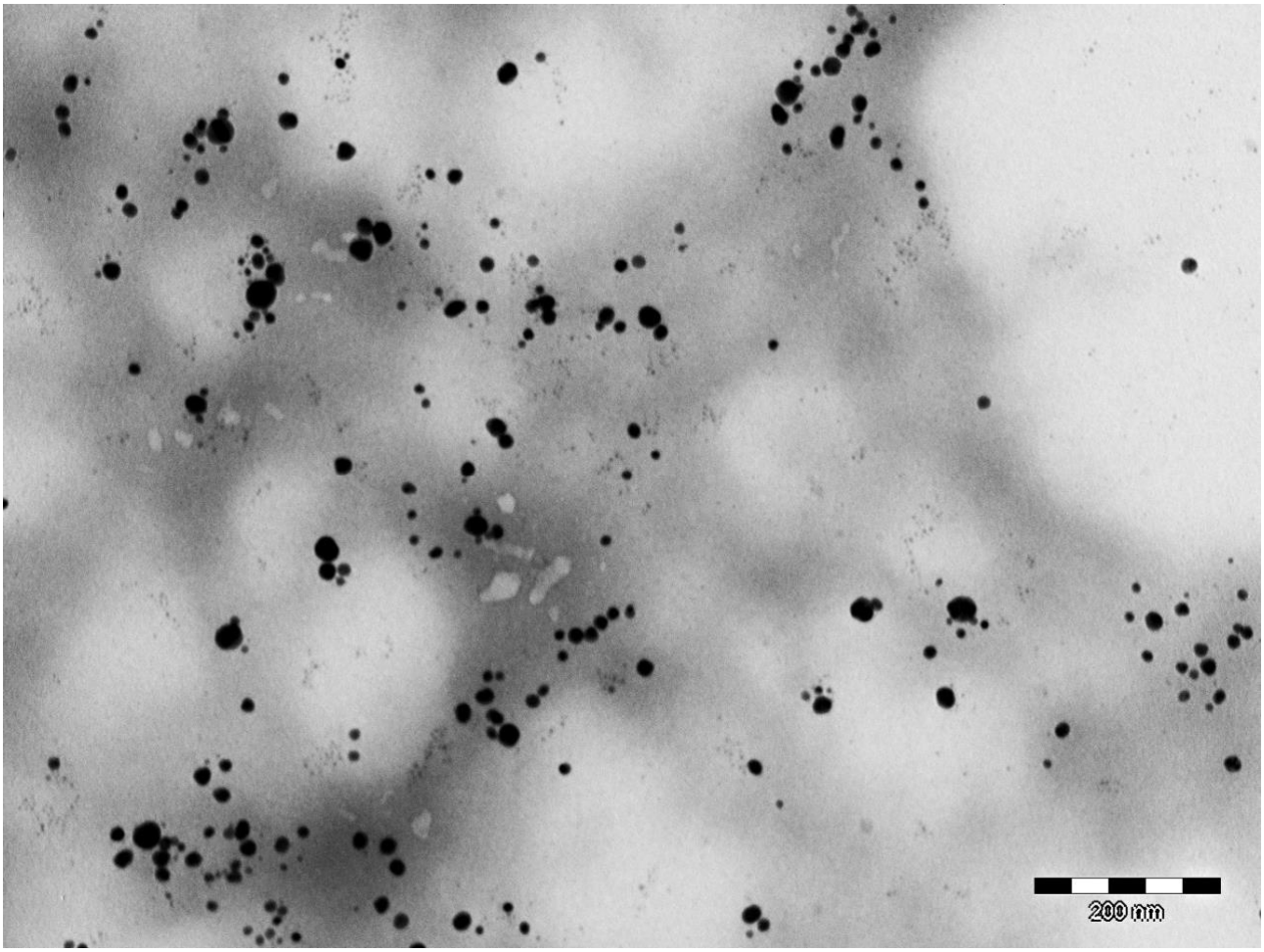

Figure SI4E: TEM image for synthesis with 0.01M Ag^+, 2.0% pectin, 60 °C

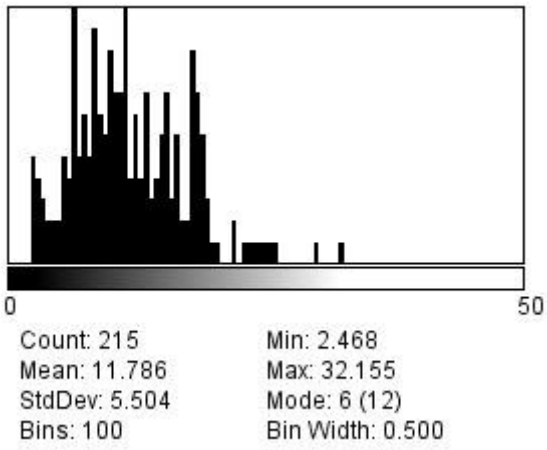

Figure SI4F: dimensional counting from the previous image

SI5 – Potentiometric determination of ionic Ag^+ in p-AgNP

The method allowed us to determine Ag(I) in pectin solutions, despite the presence of the polysaccharide. In fact, when known amounts of silver nitrate (from 0.1 up to 200 mg/L) were added to plain KNO_3 solution, 0,1%, 0,5%, 1% or 2% pectin solution, and a log [Ag^+] vs E (mV) plot was performed, a straight line with Nernstian slope (ca 60 mV for tens time change in concentration) was observed in all cases,[R1] both at <5 mg/L silver concentration and at >5 mg/L Ag^+ concentration,

without changes in the slope of the curve.[R2] A recovery >>95% of the silver added was observed in these condition by standard addition method. This prove that, as already known for the case of Ag^+ and gelatin, both the silver complexed by the macromolecule and the free ion is determined with this method.[R3] In these conditions, a LOD of 0.1 mg/L was found.

[R1]: United States Dep of Commerce, NIST,Maurice H. Stans,Lewis N. Branscomb, Ion-Selective Electrodes, Maryland, 1969, p 59 and following; p 380 and following)
[R2]: Stability constants for the complexation of copper(II) ions with water and soil fulvic acids measured by an ion selective electrode, William T. Bresnahan, Clarence L. Grant, James H. Weber, Anal. Chem., 1978, 50 (12), pp 1675–1679)
[R3]: Determination of silver in photographic emulsion: comparison of traditional solid-state electrodes and a new ionselective membrane electrode Ritu Kataky, Martin R. Bryce and Brian Johnston (Analyst, 2000, 125, 1447–1451; Known Addition Ion Selective Electrode Technique for Simultaneously Determining Fluoride and Chloride in Calcium Halophosphate Lowell G. Bruton; ANALYTICAL CHEMISTRY, VOL. 43, NO. 4, 1971 579-581

Table SI5 - % of free Ag^+ (total Ag = 0.001 M)

%pectin	0.5		1.0		2.0	
T (°C)	20	60	20	60	20	60
% Ag^+	0.946	1.34	-[a]	0.198	<0.1	0.47

[a] not determined

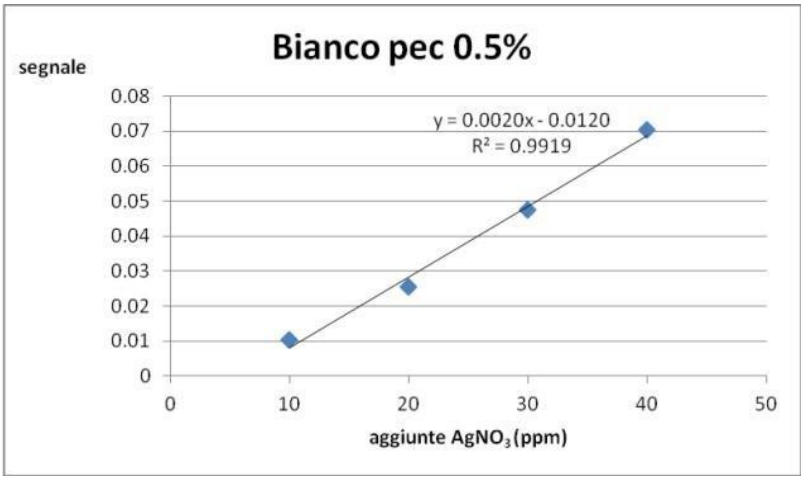

A

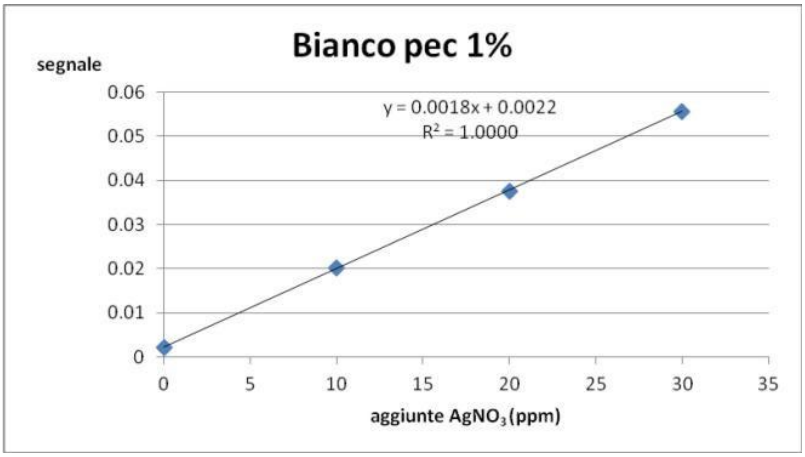

B

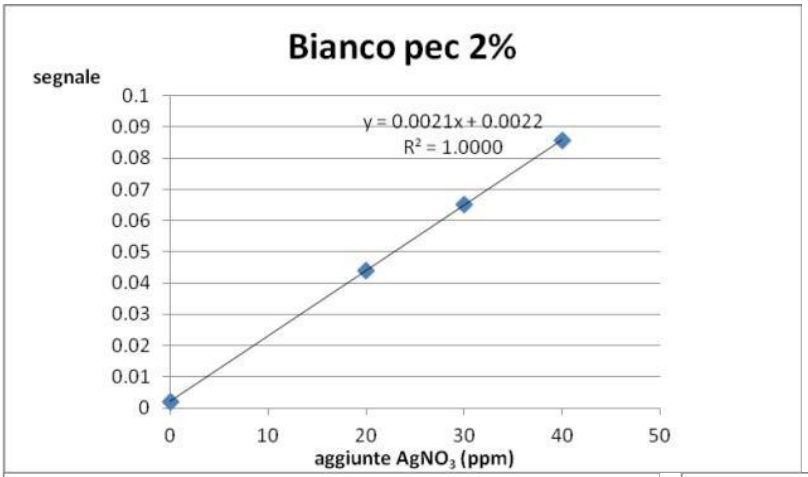

C

Figure SI5A-C. Calibration curves in 0.5% (**A**), 1.0% (**B**), 2.0% (**C**) pectin, as DPV signal intensity vs added $AgNO_3$ (in ppm)

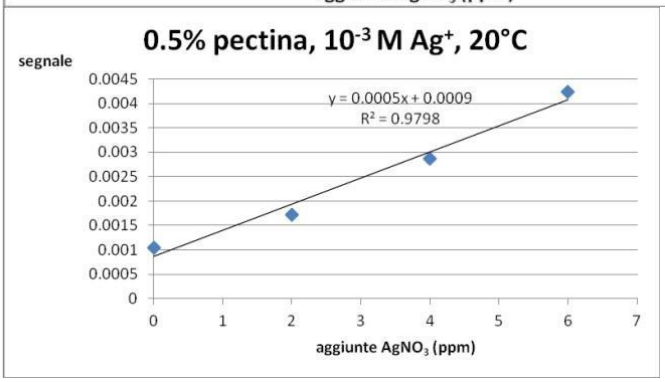

D

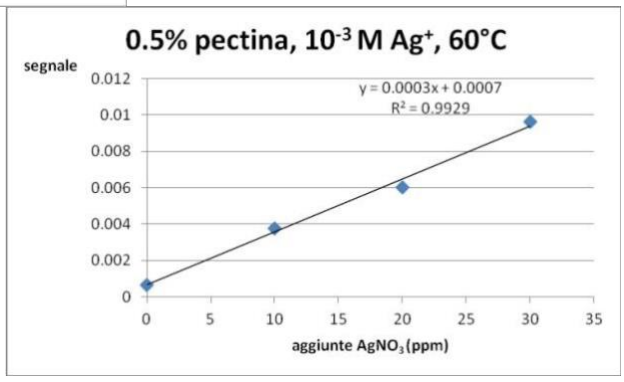

E

Figure SI5D-E: determination of free Ag^+ in syntheses with 0.001M Ag+, 0.5% pectin, carried at T = 20 °C (**D**) and 60 °C (**E**). DPV signal intensity vs added $AgNO_3$ (in ppm)

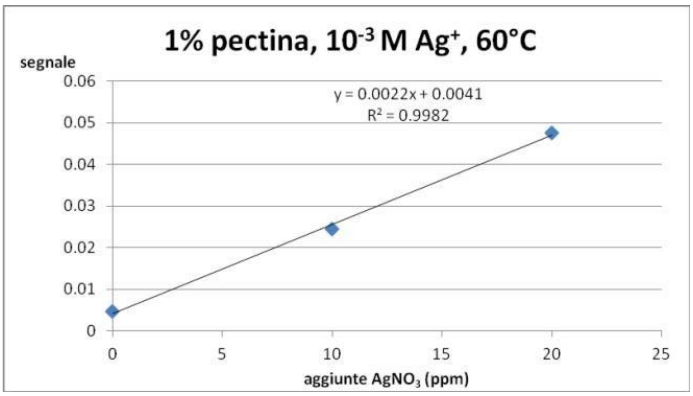

Figure SI5F: same, in 1.0 % pectin, 60 °C

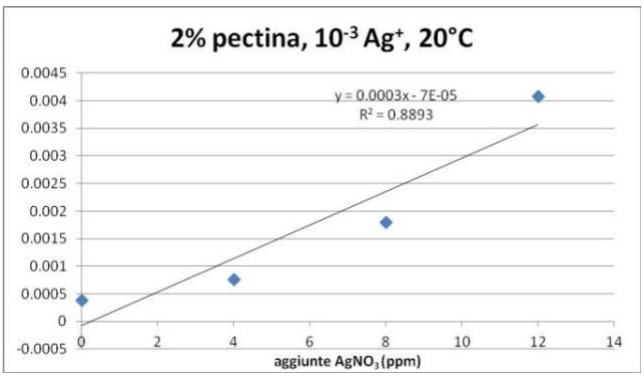

G

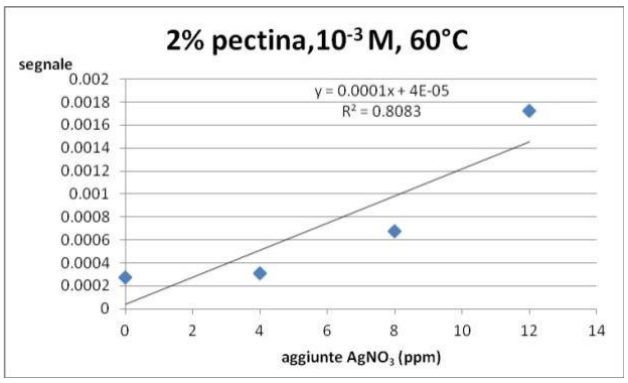

H

Figure SI5G-H: same, in 2.0 % pectin, synthesis carried out at 20 °C (**G**) and 60 °C (**H**)

SI6 – Thermogravimetric and calorimetric experiments.

SI6.1 TGA on pure pectin. Pure pectin sample's thermogravimetric analysis (Figure SI6A) shows a mass loss of about 7.3 wt % below 100 °C, that could be due to the release of the adsorbed water. Starting from 450 °C, a huger mass loss is evident, characterized by three overlapping steps with different kinetics, with the last one not yet ended at the maximum temperature reached in the measurement. At the end of the heating ramp, the total mass loss is of 95.2 wt%. The residual powder (4.8 wt%), analysed by XRPD, gives a signal characteristic of an amorphous phase and could be constituted by residual carbonaceous materials.

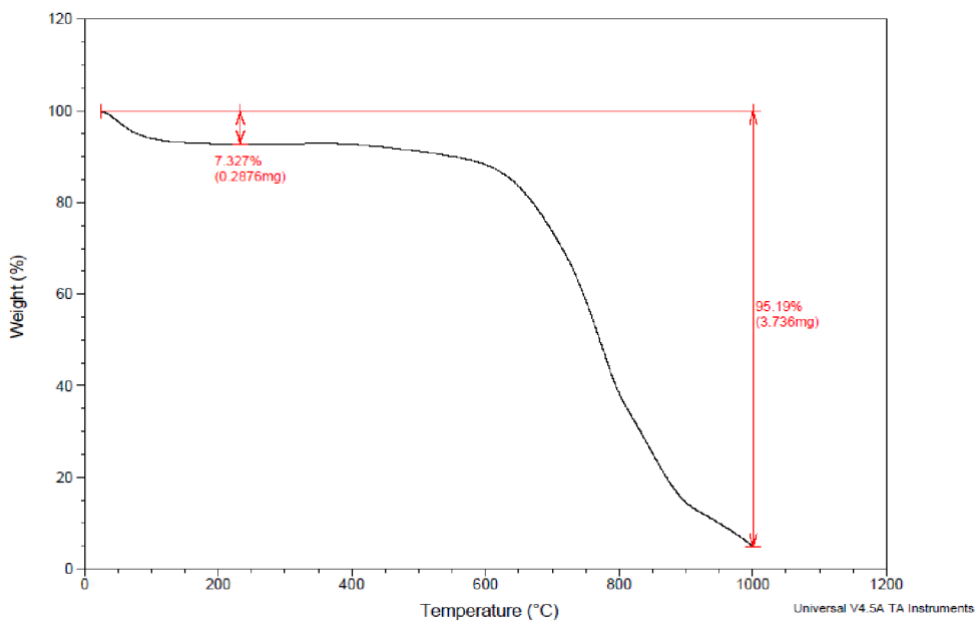

Figure SI6A . Pure pectin thermogravimetric analysis

SI6.2 TGA-DSC measurements on p-AgNPs. The thermogravimetric curve (black, Figure SI6B) shows, after the mass loss due to the water adsorbed release (about 13 %), a two steps decomposition process, with the first stage starting fast at 150 °C and ending with a very slow tail at 500 °C and the second, slower, one from 650 °C to 1000 °C. The residual mass (not constant, like for the pure pectin sample) at the end of the measurement is 8.5 wt %. Considering a residual mass loss for pure pectin of about 5 wt % (as seen in SI6.1) we can estimate an amount of metallic
Ag of 3.5 wt%.

In the calorimetric profile (blue, FigureSI6B), a more pronounced exothermic peak and a wide endothermic signal in correspondence of the beginning and the end of the first mass loss step and some small endothermic peaks underlying the second decomposition step are evident. A small endo peak with onset point at 955 °C and centered at 960 °C is evident. Being Ag a calorimetric standard melting at 961.78 °C [Metrologia, 27, 3-10 (1990)], the above quoted peak can be attributed to the melting of the small amount of metallic Ag in the preparation. Starting from the melting enthalpy of pure Ag (104.4 J/g; http://www.tainstruments.co.jp/application/pdf/Thermal_Library/Applications_Notes/TN011.PDF) and the measured enthalpy for the above descrive peak (3.5 J/g), an amount of Ag of about 3.35 wt % can be estimated, in very good agreement with the deduction made starting from TGA data. The presence of crystalline metallic Ag is confirmed also by the XRPD analysis performed on the residual powder.

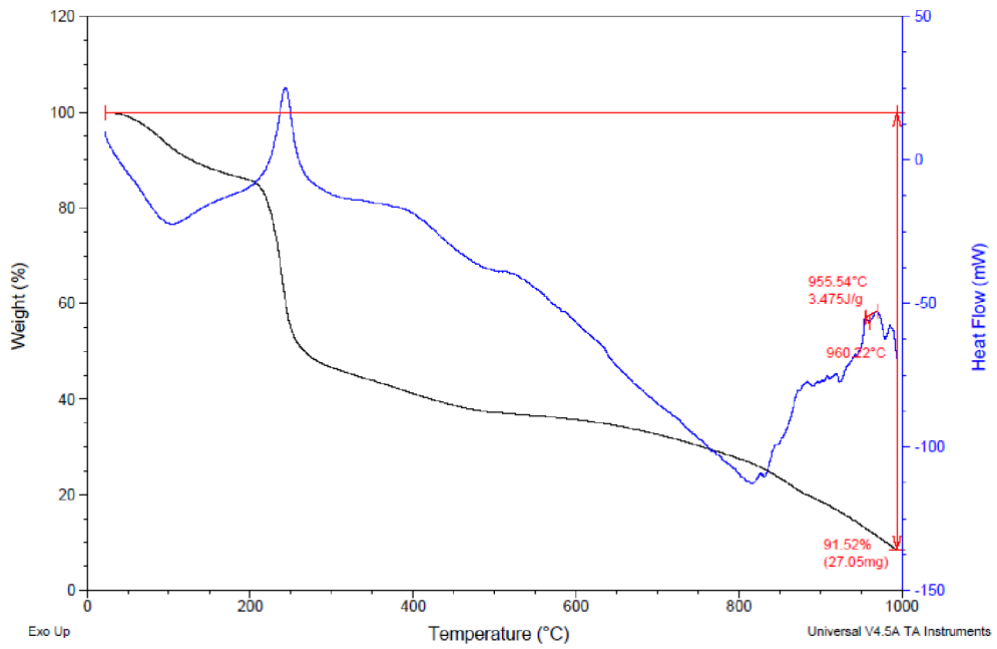

Figure SI6B. TGA (black) and DSC (blue) profiles for dry p-AgNP

SI7 – X-ray diffraction

Powder x-ray diffraction was run on samples prepared with the standard protocol (0.001M Ag^+/1% pectin/ 60°C) and 1:1 Ag/pectin molar ratio, i.e. 0.5 g pectin (2.35×10^{-3} mol of galacturonic acid) in 50 mL water, with 0.400 g (2.35×10^{-3} mol) $AgNO_3$, at pH 12, 60 °C. Powders were isolated as described in the experimental for the thermal chararcterization.

Nanocrystalline cubic silver was found in both cases (COD 1509146; spatial group F m -3 m; a = 4.071 Å; V = 67.469 $Å^3$).

We were able to determine the average crystallite dimension only in the 1:1 sample. Calculation with Debye–Scherrer formula gave 75 Å, a value confirmed also by Rietveld analysis with the MAUD program (74.5 ± 2 Å).

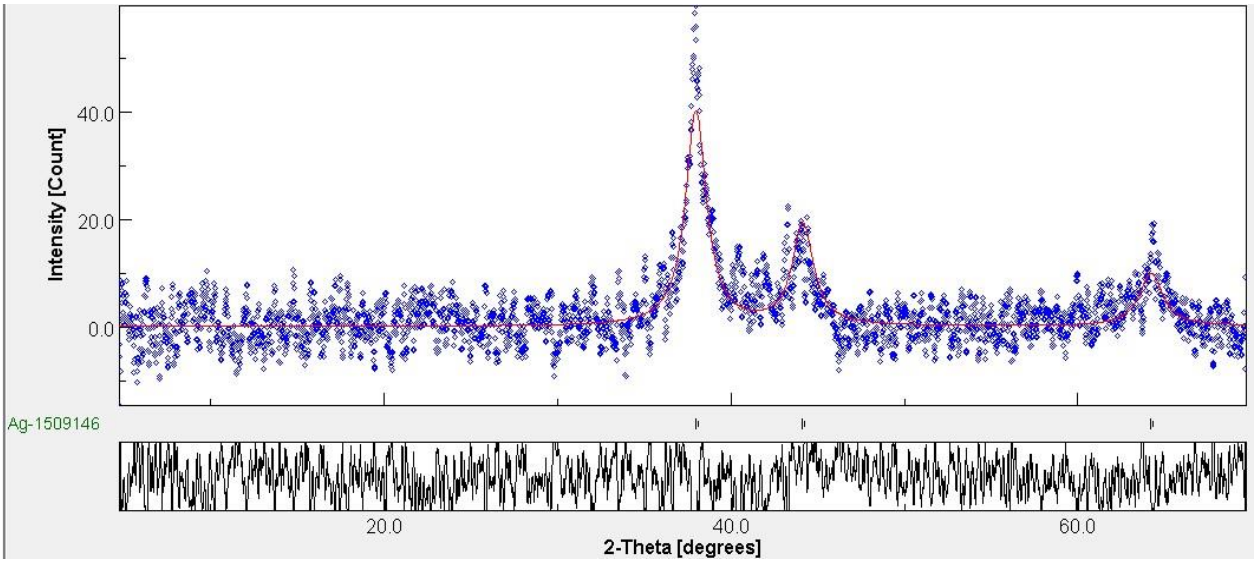

SI8 – MIC determination in liquid culture conditions (plactonic cells).

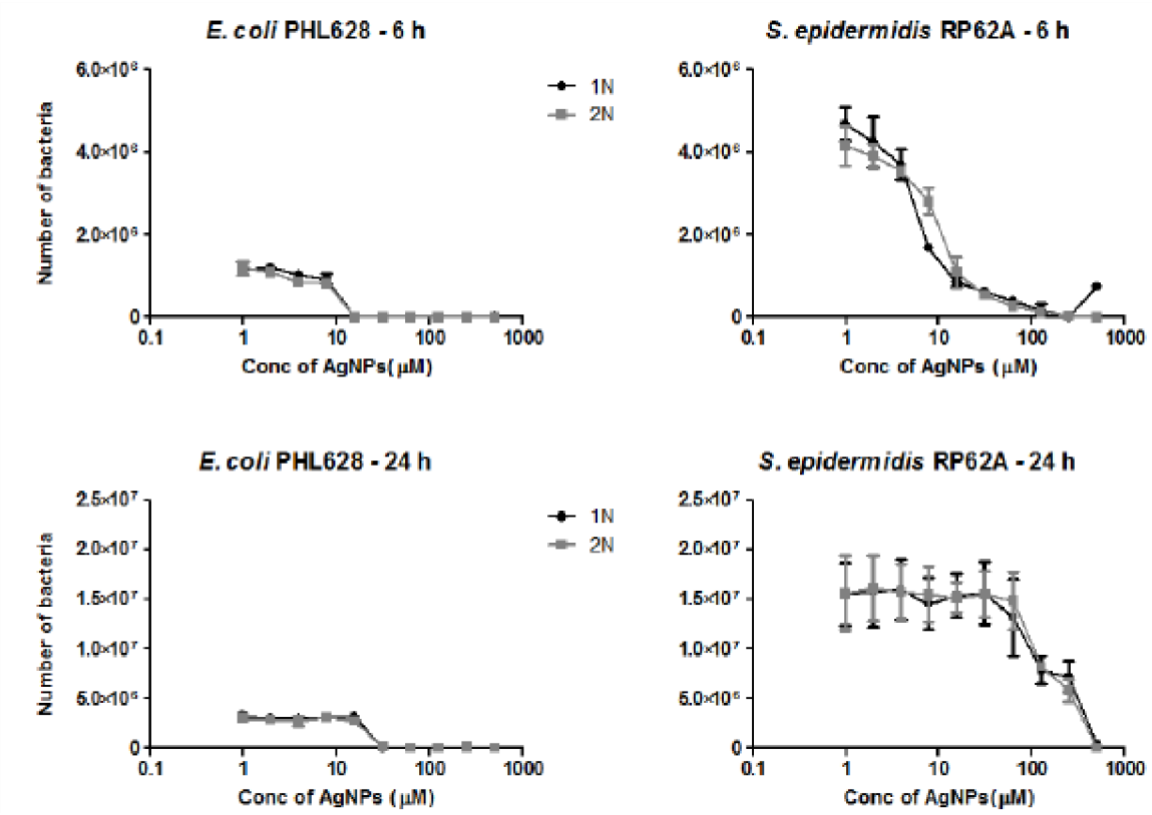

Figure SI8. Viability (number of viable bacteria) of *E. coli* PHL628 and *S. epidermidis* RP62A in liquid culture conditions at two different time points (6 hours, upper row, and 24 hours, lower row) as a function of Ag concentration from a 10^{-3}M (in Ag) p-AgNP solution

SI9. Ag^+ release.

Ag^+ concentration was measured in the 20 mL aqueous phase external to a 20 mL sample of pAgNP inside an osmosis membrane. Ag^+ was determined by ICP-OES analysis on 3.0 mL samples.

sampling time	Ag
0.5 h	0.04 mg/L
3.0 h	0.11 mg/L
24 h	1.95 mg/L

SI10 – Larger CLSM images.

Panels a-h of Figure 5 of main text are reproduced here at 200% zoom

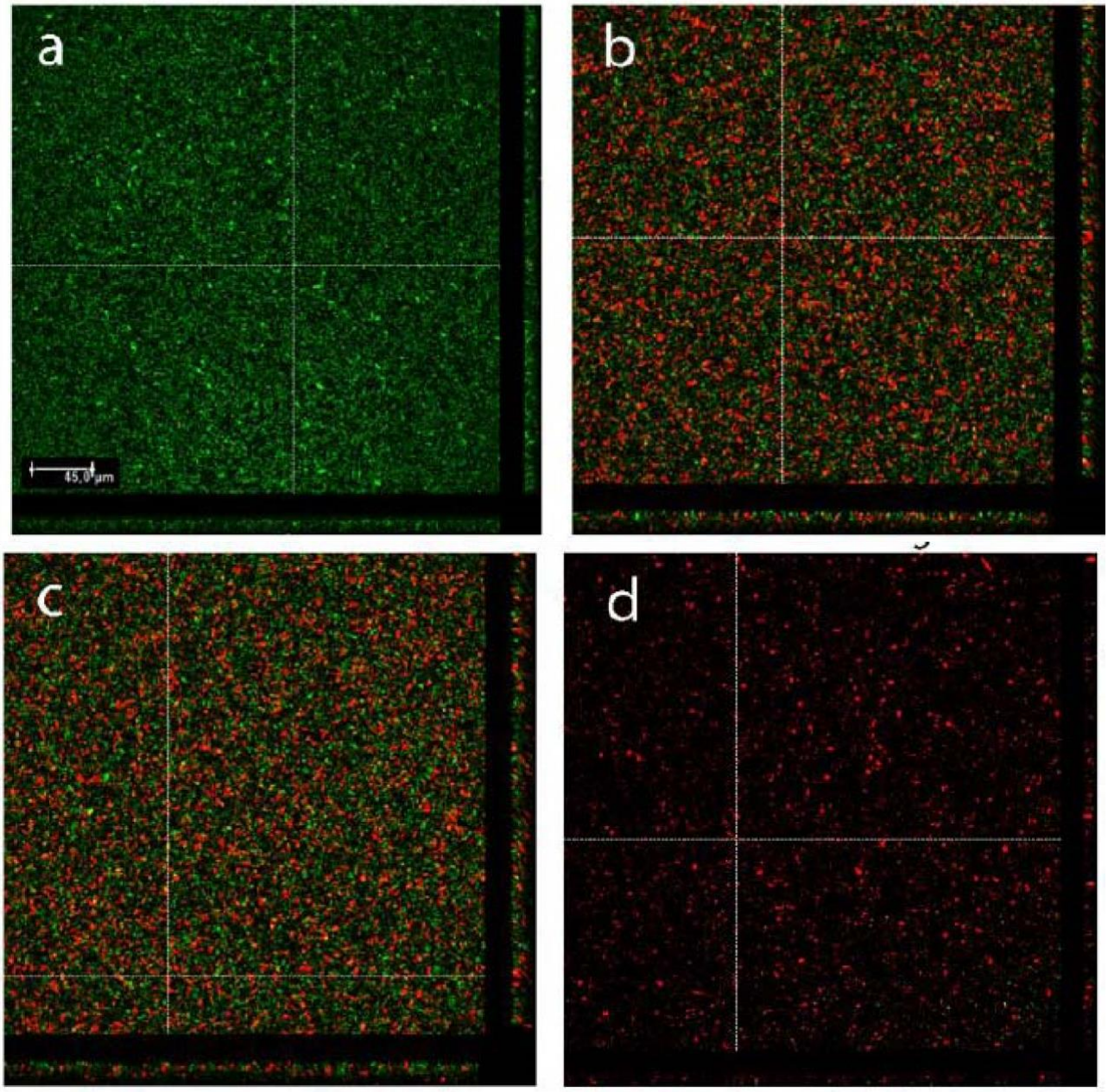
a
45,0 µm
b
c
d

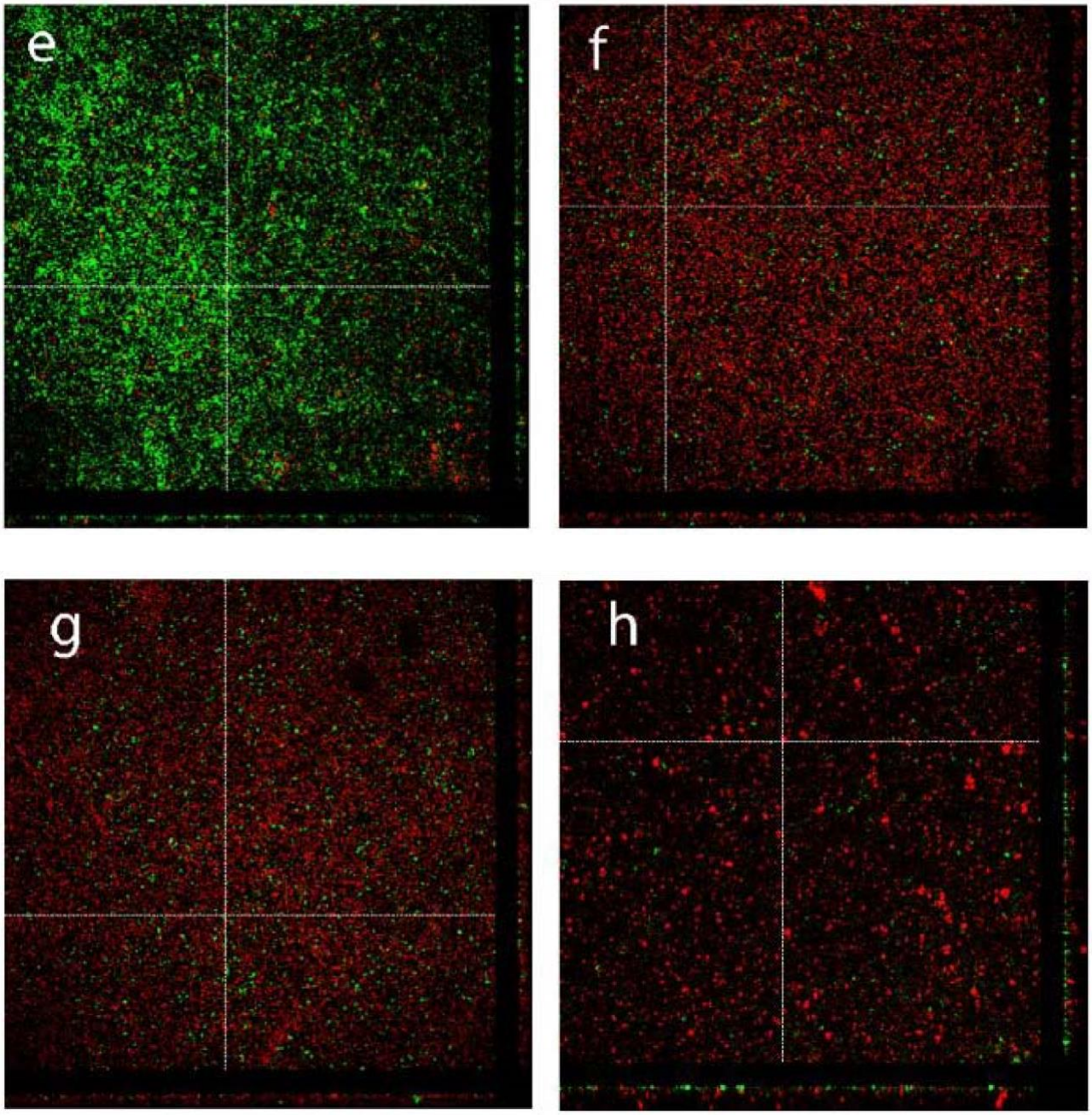

S11 – Fibroblast viability and proliferation

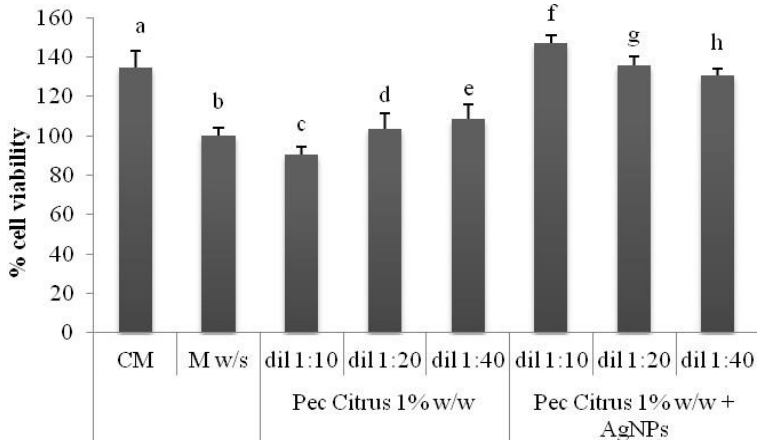

Figure S11A. Viability values of 1% pectin and p-AgNP tested at different dilutions (1:10, 1:20 and 1:40 (v/v)). CM and M (w/s) were used as reference (mean values ± s.e.; n=8). Anova one way – Multiple Range Test ($p<0.05$): a vs b/c/d/e; b vs f/g/h; c vs f/g/h; d vs f/g/h; e vs f/g/h; f vs h.

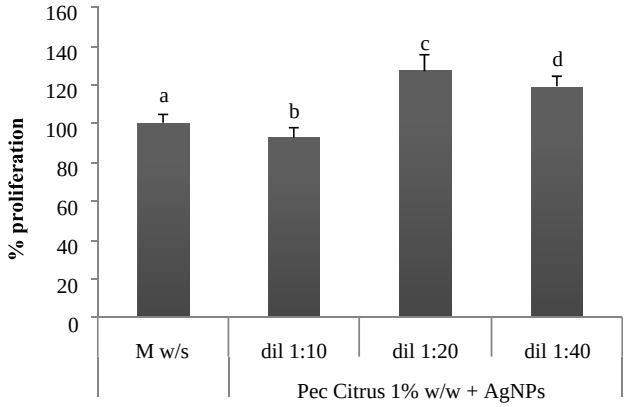

Figure S11B. % proliferation values in the presence of p-AgNP. M (w/s) was used as reference (mean values ± s.e.; n=8). Anova one way, MRT ($p < 0.05$): a *vs* c/d; b *vs* c/d